# Resonance Raman spectroscopy and its application in bioinorganic chemistry

Wesley R. Browne

Molecular Inorganic Chemistry, Stratingh Institute for Chemistry, Faculty of Science and Engineering, University of Groningen, Nijenborgh 4, 9747 AG, Groningen, The Netherlands

#### **Abstract**

This chapter introduces the Raman spectroscopy and the concept of resonance enhancement of Raman scattering. The first part introduces the fundamentals of vibrational spectroscopy and explains key terms such as dipole moment and the dipole operator. The discussion of the resonance Raman experiment and practical aspects is followed by details of the underlying theories that explain the resonance enhancement effect. A short discussion of surface enhanced Raman spectroscopy is followed by examples of the use of resonance Raman spectroscopy and finally time resolved (excited state) Raman spectroscopy is discussed briefly.

### **Table of Contents**

Resonance Raman spectroscopy and its application in bioinorganic chemistry	1
1 Introduction	4
2 The fundamentals of vibrational spectroscopy	4
2.1. The classical oscillator, Hooke's law, the force constant and quantization	6
2.2. Quantization and the nature of a quantum excitation	8
3 Permanent, induced and transition electric dipole moments	10
3.1. Electric dipole moments	10
3.2. Transition dipole moments	11
3.3. Polarizability, induced dipole moments, and scattering	12
3.4. What is $\varphi vf *x \varphi vidx$ ?	15
3.5. Relative intensities of Stokes and anti-Stokes Raman scattering	16
3.6. What is a virtual state?	16
4. The (resonance) Raman experiment	17
4.1. Raman cross-section and the intensity of Raman bands	20
4.2 Raman scattering is a weak effect; but how weak?	21
5. Resonance enhancement of Raman scattering	22
5.1. The Raman spectroscopy of carrots and parrots	23
5.2 Classical description of Rayleigh and Raman scattering	25
5.3. The Kramer-Heisenberg-Dirac (KHD) equation	26
5.4. A-, B-, C-term enhancement mechanisms, overtones and combination bands	28
5.5. Assigning electronic absorption spectra	29
5.6. Heller's time dependent approach	31
6. SERS and SERRS spectroscopy	33
7. Experimental and instrumental considerations	34
7.1. Isotope labelling and band assignment	34
7.2. Resolution and natural line width	36
7.3. Confocality, the inner filter effect, and quartz	36
8. Applications of resonance Raman spectroscopy	38
8.1. Resonantly enhanced Raman spectroscopy in the characterization metalloenzymes based on the LmrR protein	
8.2. Reaction monitoring with resonance Raman spectroscopy	40
8.3. Transient and time resolved resonance Raman spectroscopy	40
9. Conclusions	42
10 Questions	40

11. Acknowledgements	45
12. References	45

#### 1 Introduction

The inelastic scattering of light was predicted by Adolf Smekal in 1923 and the experimental observation of this phenomenon, by C.V. Raman, was reported in the journal Nature in 1929. The award of the Nobel Prize in Physics in 1930 recognised the immediate importance of the discovery, however, it was not until the early-1990s that the instrumentation necessary to record Raman spectra routinely became available; especially sensitive detectors, steep Rayleigh scattering rejection filters, and high quality monochromatic lasers. These technical developments moved the technique from 'home-built' systems in physical laboratories out to the wider world of chemistry laboratories, and more recently first responders, factories, hospitals and airports, as a widespread analytical tool. Despite the rapid advances in laser and detector technology, and that Raman spectroscopy is now affordable (affordable hand held devices are now available), it is still the case that it is often perceived as being a somewhat exotic or specialist tool. This perception is in part due to the long delay between discovery and routine application that is in sharp contrast to the development of the related technique, Fourier Transform Infrared (FTIR) spectroscopy.

Raman spectroscopy is a highly adaptable spectroscopic technique requiring no or at least minimal sample preparation. In comparison with FTIR spectroscopy, the spectra have well resolved bands and are simpler because overtones and combination bands are generally weak or absent. Furthermore, the instrumentation used for Raman spectroscopy is relatively uncomplicated – indeed a Raman spectrometer is essentially a spectrofluorimeter on which one records emission spectra but with very high wavelength resolution! Indeed, it is of note that the intensity and signal to noise (S/N) ratio of the Raman band of water at 3500 cm<sup>-1</sup> is typically used as a figure of merit for spectrofluorimeters.

Raman scattering is an incredibly improbable phenomenon, however, when the wavelength of the laser used coincides with the wavelength of an electronic absorption band of a molecule, the intensity of the Raman scattering can increase by many orders of magnitude. Spectra obtained under this condition are referred to as a resonance Raman spectrum and can allow species present at as low as micromolar concentrations to be observed and studied. The phenomenon of resonance enhancement has made Raman spectroscopy a key technique in bioinorganic chemistry especially. Although it may be perceived as a highly specialised technique, as we will see, in practice recording a 'resonance Raman' spectrum is no different to recording a non-resonant 'normal' Raman spectrum. In fact, the only practical distinction between a Raman spectrum and a resonance Raman spectrum is the choice of wavelength of laser used and consideration of inner filter effects. Both of these aspects will be discussed below.

In this chapter, we will first introduce the basis for vibrational spectroscopy and instrumentation used to record a (resonance) Raman spectrum, and thereafter, superficially, the theory of (resonance) Raman spectroscopy. We will then consider the phenomenon of resonance enhancement of Raman scattering. A brief discussion of the various sampling aspects that are relevant to (bio)inorganic chemistry will be given, before finally, a number of examples will be described to illustrate both the simplicity and possibilities this technique presents to (bio)inorganic chemistry.

#### 2 The fundamentals of vibrational spectroscopy

Before discussing resonance enhancement of Raman scattering (known colloquially as resonance Raman spectroscopy or rR), it is necessary to consider first what a 'vibration' is, and the nature of the interaction of electromagnetic radiation (EM) with matter.

When we think of electromagnetic radiation, we usually think of photons; packets of energy that fly through space. However, they are much more than quanta of energy. Photons carry information in the form of angular momentum and specifically one quantum of angular momentum. The concept that photons have momentum (p) related to their wavelength ( $\lambda$ ) arises from the de Broglie relation  $(p = h/\lambda)$ . Furthermore, a photon has an electric and magnetic field that, to the observer from the side, appears to oscillate ( $E_{(t)} = E_o \cos(\omega t)$ , where  $E_o$  is the amplitude and  $\omega = 2\pi v$ , is angular frequency) in the direction of propagation. The electric and magnetic components rotate about the axis of propagation when viewed down that axis. In addition to the interaction of the oscillating electric field with the electrons and nuclei in the substance, the transfer of angular momentum of the photon needs to be taken into account also when considering the mechanisms by which a photon interacts with matter. In routine spectroscopy, we need also to consider the flux (number per unit time) of photons, as it is the total electric field (combination of the fields generated by each photon) that interacts with dipoles and charged particles. In the case of electrons and nuclei the response is dependent on the frequency of the light. With mid-infrared (IR) light the frequency of oscillation of the photons is close to that of nuclear oscillation (motion) while the frequency of visible and Near Infrared (NIR) photons is much higher and corresponds to the frequency at which electrons in molecules will oscillate.

When UV/visible and NIR light impinges on matter, the electric field varies over time and the electrons move resonantly (oscillating with the same frequency) with the nuclei remaining at their positions creating an induced dipole moment through the creation of regions of excess negative and positive charges (Figure 1). In this simple model, we assume that the Born Oppenheimer approximation holds; nuclei are essentially static on the time scale of these processes and only the electrons are affected by the interaction with light. We will see later with the Heller formulism that this is not exactly true. The oscillating motion of the electrons (i.e. accelerating and decelerating charge) in turn generate electromagnetic radiation with precisely the same frequency of the light used to excite them, which is termed scattered radiation. Rayleigh scattering is the dominant process and its wavelength dependence  $(1/\lambda^4$ , see below) gives rise to the blue colour of the sky – blue light is scattered more easily than red light. It is important to note that the scattering refers to the fact that the generated Rayleigh scattered light travels in all directions and should not be confused with Mie scattering (i.e. scattering due to particles with dimensions close to that of the wavelength of the light used).

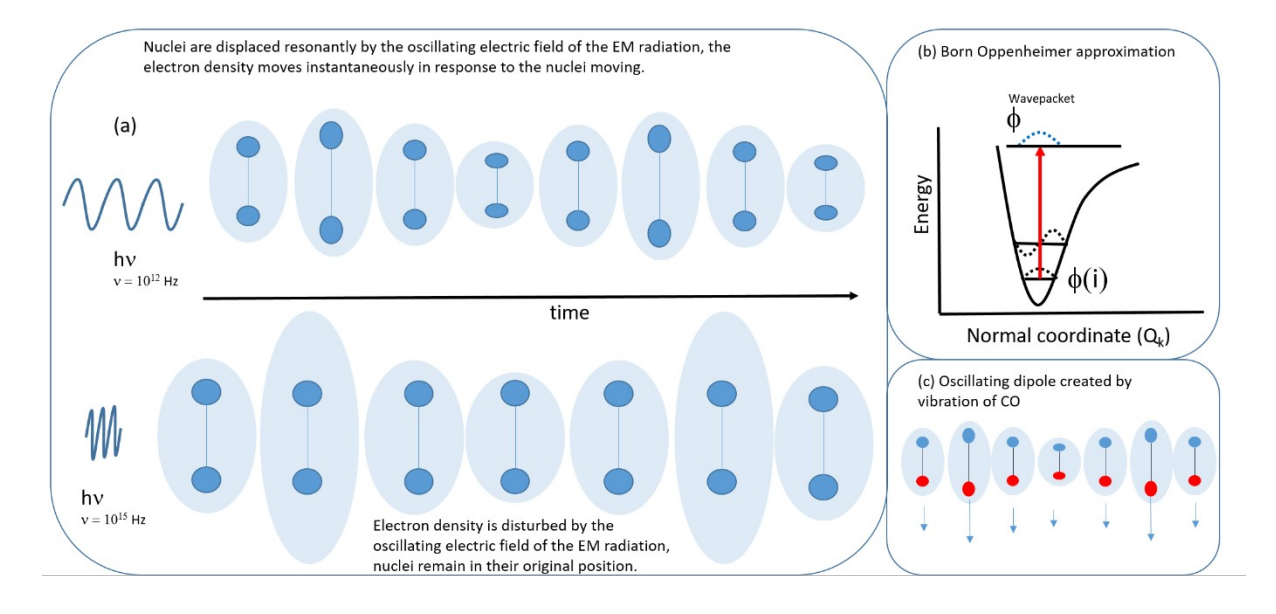


Figure 1. (a) Interaction of electromagnetic radiation ( $E = hv = hc/\lambda$ ) with electrons and nuclei. For light at lower energy (frequency, the IR region), the nuclei oscillate under the influence of light and the electrons respond instantaneously to the change in nuclear position (upper part). In contrast, light in the UV/vis frequency range will induce oscillation of the electrons only, and the nuclei will remain at their equilibrium positions (lower part). (b) The Born Oppenheimer approximation; electrons move on a time scale much shorter than nuclei and hence an electric field created by light in the UV/vis region will distort the electron 'cloud' around nuclei raising the energy of the molecule but without changing the coordinates of the nuclei and hence the nuclear wavefunction (wavepacket). (c) Oscillating dipole created by a molecular vibration.

In IR spectroscopy, the energy of a photon is absorbed, resulting in excitation from the lowest vibrational state  $(\varphi_i)$  to a higher energy state  $(\varphi_f)$ . The energy of the photon (E = hv) must equal the difference in energy between the two vibrational states, i.e. it must be resonant. For the transition to occur, there must be a change in dipole moment between the two states, which is represented by the transition dipole moment  $(\vec{\mu})$  and the transition dipole moment operator  $(\hat{\mu})$ . The transition takes place because the nuclei oscillate at the similar frequencies of the light impinging on them (i.e. in the infrared region, ca.  $10^{12}$  Hz).

The interaction of the oscillating electric field of light at much higher frequencies (UV, visible and NIR light) either:

- induces movement of electrons, which in turn delays propagation of the wave (this is the real component of the refractive index/dielectric constant of a material)
- results in the absorption of the energy of the photon (absorbance)
- change the direction of propagation (Rayleigh scattering)
- occasionally result in the photon losing or gaining energy (Raman scattering)

Although the interaction of a photon with matter is easiest thought of as the molecule absorbing the energy of the photon, this can only happen if a number of conditions are satisfied – the most important of which are resonance and the conservation of angular momentum. However, the electrons in a molecule interact transiently with the electric field created by the photons without absorbing their energy. Instead the molecule is excited to a virtual state, from which it generates a photon of the same frequency as the incident light as the electrons move back to their original positions. Note that an oscillating charged species will generate electromagnetic radiation. We will discuss the details of this in depth below.

## 2.1. The classical oscillator, Hooke's law, the force constant and quantization

The basis of vibrational spectroscopy has its roots in the study by Robert Hooke in the 17<sup>th</sup> century of oscillators, such as the motion of pendulums, and masses connected by springs. From a classical perspective, we can think of a simple molecule such as dihydrogen (H-H) as two point masses (the nuclei) that are subject to forces.

- The first force is the due to the mutual repulsion of positively charged nuclei. The repulsion between positively charged nuclei means that it energy is used to bring the nuclei together. The energy is stored in as potential energy (PE).
- The second force is the attraction of the nuclei to the shared electrons and the closer the nuclei are, the closer they are to the electrons also and hence their potential energy is lowered (i.e. separating the electrons and nuclei takes energy).

Together these two interactions give rise to the London dispersion forces. If at some distances the net result is a decrease in potential energy (i.e. the electron nuclear attraction is greater than the internuclear repulsion) then a stable situation is realized (Figure 2). The range of distances over which the attraction outweighs the repulsion is relatively narrow and the bottom of the well has approximately the shape of a parabolic curve; a feature that is made good use of in the mathematical descriptions below.

In cartoon fashion we can think of a bond as being two atoms connected by a spring (Figure 2a). In the classical (Newtonian) world two properties of oscillators make immediate sense. The oscillator can be at rest (i.e. the pendulum is not swinging, balls connected by a spring are not moving) or if the oscillator is in motion (oscillating) then, given any momentary observation in time, it is most likely (maximum probability) that it will be at the extreme points of the oscillation (since it is moving the slowest, lowest kinetic energy/highest potential energy at these points).

If the angle through which the oscillation takes place is small, then pendulums (oscillators) always swing (oscillate) at a set frequency. The oscillation frequency is dependent only on their length (Figure 2a). For masses connected by a spring, however, the stiffness of the spring and the effective mass determine the frequency of oscillation (Figure 2b). These observations led Robert Hooke to establish what became known as Hooke's law.

$$v_{\rm osc} = \frac{1}{2\pi} \sqrt{\frac{k}{m_{\rm eff}}}$$

Where  $v_{osc}$  is the natural frequency of the oscillator (usually expressed in wavenumbers, cm<sup>-1</sup>) and is proportional to the force constant k (a measure of the strength of a bond) and inversely proportional to the effective mass ( $m_{eff}$ ), which for a two atom oscillator (figure 2c) is equivalent to the reduced

$$\max \left( \mu = \frac{m_1 m_2}{m_1 + m_2} \right).$$

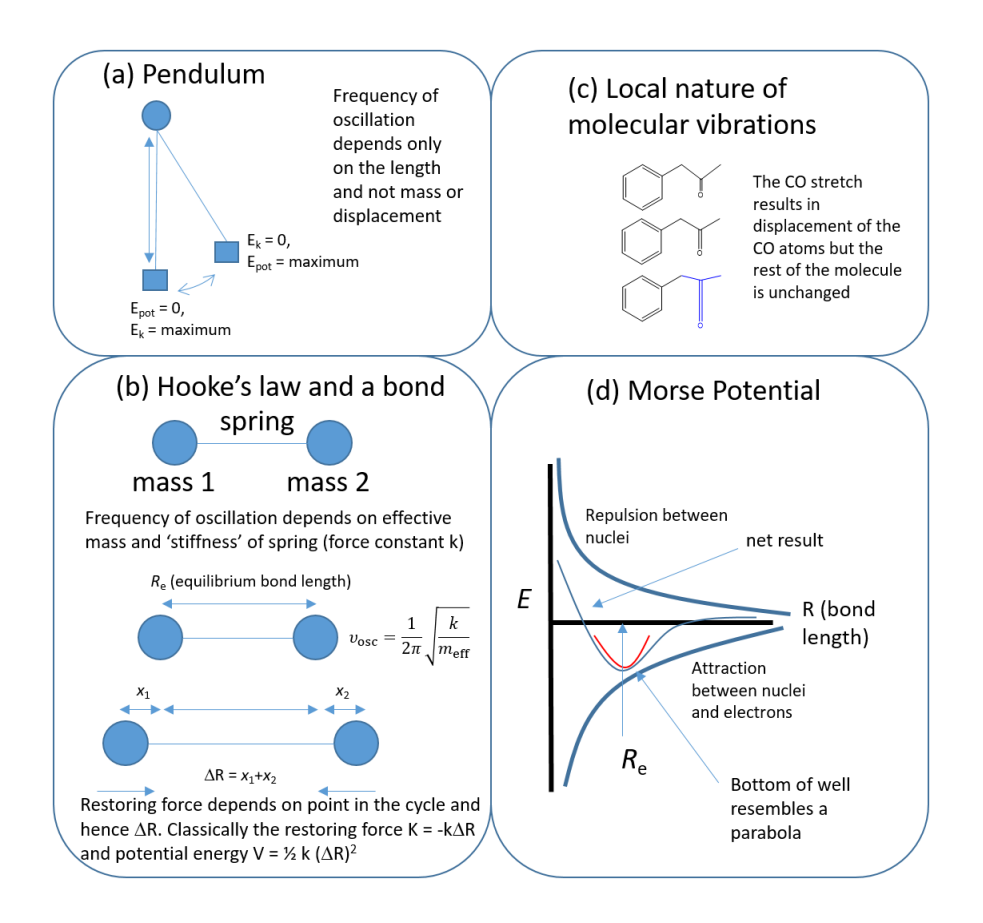


Figure 2. (a) The pendulum. PE = potential energy, KE is kinetic energy. (b) Hooke's law and the spring connecting two balls model of a chemical bond. (c) Local nature of vibrations. (d) Morse potential well formed by competition between internuclear repulsion and electron nuclear attraction. If the net result is a minimum (bonding interaction) then the minimum is the equilibrium bond length and the region around it approximates a parabolic curve.

The restoring force K exerted on the atoms that are oscillating depends on the point in the oscillation that the system is at, i.e. the restoring force is greatest when  $|\Delta R|$  is at a maximum and zero when  $|\Delta R| = 0$  (Figure 2c). Indeed K = -k  $\Delta r$  and the potential energy is  $E = \frac{1}{2} k x^2$  (where  $x = \dot{c} \Delta R \vee \dot{c}$ ), which happens to be a formula for an upward opening parabola (Figure 2d). The stiffness of the bond is reflected in the magnitude of k (the force constant); the greater k is, the stiffer (stronger) the bond is and the lower the amplitude and greater the frequency of oscillation.

#### 2.2. Quantization and the nature of a quantum excitation

A particle, such as a molecule, is in a particular energy state and position, which can be described by a wavefunction. Changing the molecule to a different state (i.e. different energy and/or position) requires that an operation is carried out. Although macroscopically we think of moving position or changing energy as a continuous process, at the microscopic level the changes are quantized and changing the energy of an entity (be it electronic, nuclear, vibrational or rotational – but not translational!) can only be done in discrete steps. It should not be forgotten that quantization, in quantum mechanics, is enforced by the imposition of a boundary. Only wavefunctions that satisfy the boundary conditions are allowed. In the case of translational motion, the boundaries are so far apart compared to the wavelength of the particle (de Broglie) that changes in energy can be

considered continuous. The vibrational energy in molecules is quantized, however, due to the confinement imposed by the potential well.

In mathematical terms we describe the transition between states using an integral as follows.

$$\int \psi_f \hat{\mu} \psi_i d\tau$$

where  $\psi_f$  is the wavefunction describing the final state,  $\psi_i$ the initial state and  $\hat{\mu}$ is the transition dipole moment operator (the mechanism by which a species changes from one state to another). It is the dipole moment operator that describes (reading left to right) how the final state is arrived at from the initial state. The integral is over all space since the wavefunctions describing each state are continuous over all space  $\tau$ . However, typically for vibrational spectroscopy we consider the wavefunction along a single coordinate, especially where a bond elongation and contraction is all that is of concern to us (Figure 3).

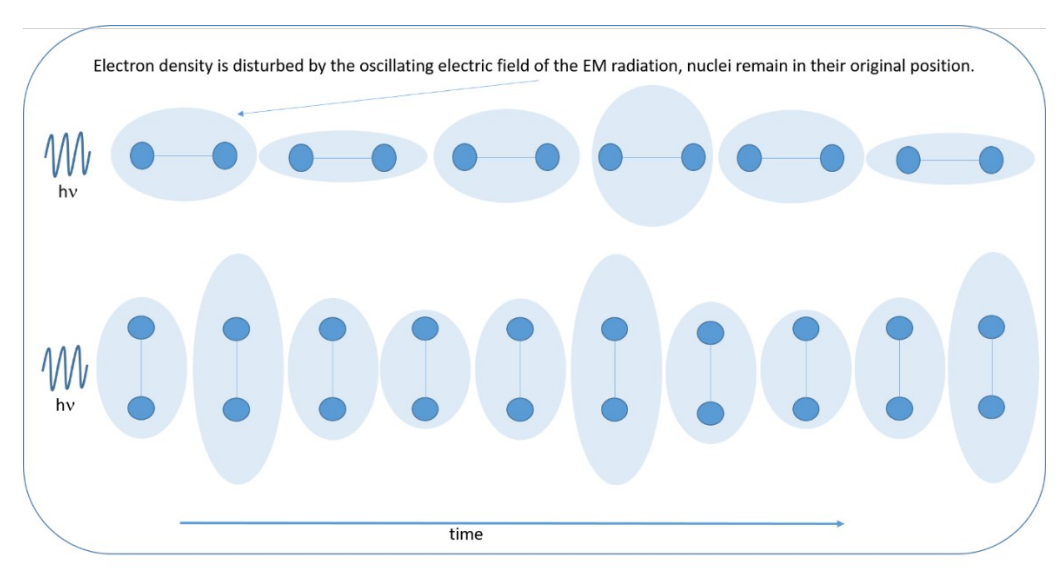


Figure 3. Interaction of plane polarized (along y-axis) light with a CI-CI bond.

A quantum mechanical oscillator can only exist in any of a series of discrete states with energies:

$$E_{vib} = h v_{osc} \left( v + \frac{1}{2} \right) = \frac{h}{2\pi} \sqrt{\frac{k}{m_{eff}}} \left( v + \frac{1}{2} \right)$$
 where  $v = 0, 1, 2, ....$ 

<insert Figure 4 here>

Figure 4. Potential well for a Harmonic oscillator with allowed quantum states equally spaced in energy and shape of Hermitian based wavefunctions. The total energy is the sum of the kinetic energy and potential energy ( $E_{vib} = E_K + PE$ ). The shape of the stationary wavefunctions that describe each vibrational level are given by the Hermitian polynomials (see below) and as the energy increases the oscillations begin to resemble the behavior of a macroscopic oscillator, with the oscillator spending most its time at the extremes of the oscillation.

The time independent Schrodinger equation:

$$\frac{-\hbar^2}{2m_{eff}}\frac{d^2\psi}{dx^2} + \frac{1}{2}k_f x^2 \psi = E\psi$$

allows us to calculate the total energy of an oscillator  $(E_{vib})$  as a sum of its kinetic and potential energy (Figure 3). The potential depends on how much  $(|\Delta r| = x)$  longer or shorter the bond is compared with the equilibrium length of the bond (the length that corresponds to the minimum of the potential well, x=0). The potential varies with separation smoothly (continuous curved function) which can be modelled using a Taylor series. And hence the potential at any distance, i.e.  $V_{(x)}$ , from the minimum can be estimated by:

$$V_x = V_{x=0} + \left(\frac{dV}{dx}\right)_{x=0} x + \frac{1}{2} \left(\frac{d^2V}{dx^2}\right)_{x=0} x^2 + \dots$$

The first term  $V_{(x=o)}$  is the potential at the equilibrium bond length (and the bottom of the well) and can be arbitrarily set to zero since it is the minimum. The potential well's curvature approximates a parabolic curve near the minimum and hence the second term  $\left(\frac{dV}{dx}\right)_{x=o}^X$  is also zero since the slope of the tangent at the minimum of an upward opening parabolic curve is by definition zero when x=o. The third term is therefore the first non-zero term:

$$V_{x} = \frac{1}{2} \left( \frac{d^{2}V}{dx^{2}} \right)_{x=0} x^{2}$$

and it corresponds to the rate of change of the rate of change of potential at the minimum.

For small displacements from the equilibrium bond length, the higher terms are negligible and hence the force constant that appears in Hooke's law  $(k_{\rm f})$  can be replaced by  $\left(\frac{d^2V}{d\,x^2}\right)_{x=o}$ : indeed this is the formal definition of the force constant (Figure 5).

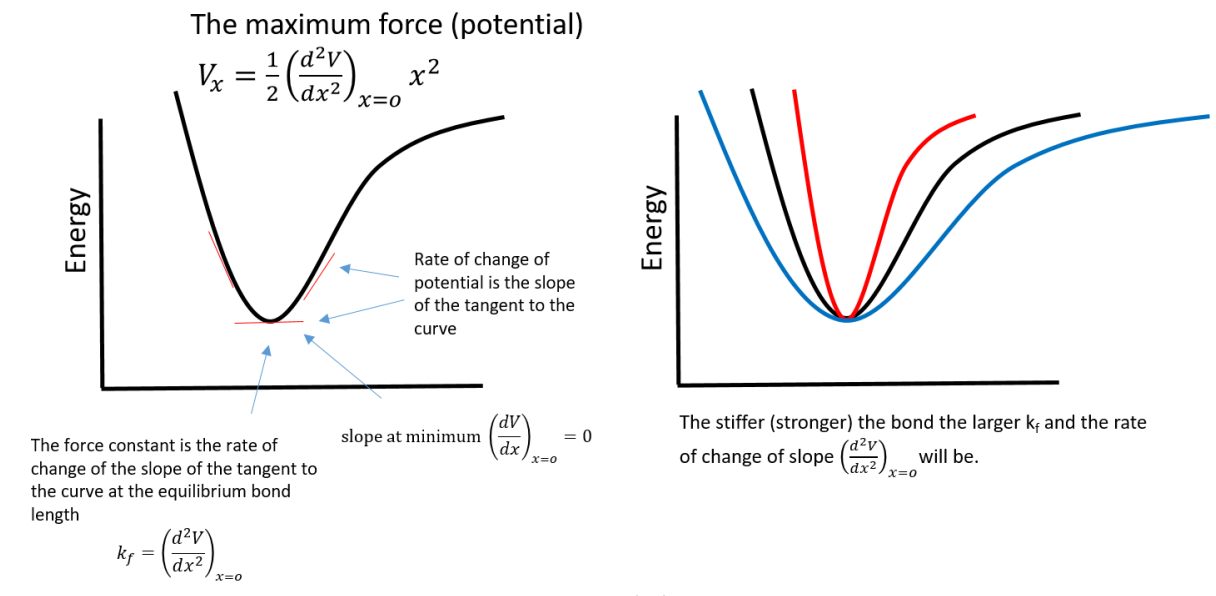


Figure 5. The formal definition of the force constant  $(k_f)$ . The stronger a bond is less the amplitude of the oscillations and the narrower the potential well will be. The rate of change of the slope of the curve  $(\frac{d^2V}{dx^2})_{x=0}$ ) increases as  $k_f$  increases.

Although the vibration of a bond in a molecule can be modelled as a harmonic oscillator, in reality the potential well is anharmonic since the bond must always be a positive distance (i.e. the separation between atoms must be greater than zero) and the bond cannot be infinitely long, as beyond a certain length the bonding interaction is negligible, as is the restoring force. However, at ambient temperatures the amplitude of the oscillations are small and the behavior of two bound atoms approximates, albeit not exactly, that of a harmonic oscillator.

#### 3 Permanent, induced and transition electric dipole moments

The following sections are somewhat of an aside from our discussion of vibrational spectroscopy, however, for a detailed discussion of the phenomenon of resonance enhanced Raman scattering, it is pertinent to first remind ourselves of some basic concepts related to the interaction of electromagnetic radiation and matter. We begin with the concept of permanent electric dipole, transition dipole and then induced dipole moments to build a basis for understanding Raman spectroscopy.

#### 3.1. Electric dipole moments

When two monopoles of opposite charge are in proximity they will generate a moment (a force) called an electric dipole moment ( $\mu$ ) between them. The strength of this dipole moment is macroscopically given by the charge multiplied by the distance by which the two charges are separated by ( $\mu = qR$ ). The electric field generated by the two charges is given by:

$$\vec{E} = \frac{1}{4\pi\varepsilon_0} \frac{\vec{\mu}}{R^2}$$

where R is the distance between the two charges and  $\varepsilon_o$  is the vacuum permittivity.

Since the potential well for the oscillator is parabolic, we can calculate the dipole moment  $\mu$  using a Taylor expansion as we did for the dipole moment in section:

$$\mu = \mu_o + \left(\frac{d\mu}{dx}\right)_{x=o} x + \frac{1}{2} \left(\frac{d^2\mu}{dx^2}\right)_{x=o} x^2 + \dots$$

Where  $\mu_o$  is the dipole moment at the equilibrium bond length and is a constant, and  $\left(\frac{d\mu}{dx}\right)_{x=o}$  is the rate of change of dipole moment at the equilibrium bond length etc.

Since we can measure the electric dipole moment (it is an observable) then in quantum mechanics, we can assign a dipole moment operator  $\hat{\mu}$ , which describes how the change in dipole moment between the initial and final states and:

$$\hat{\mu} = \mu_o + \left(\frac{d\mu}{dx}\right)_{x=o} x + \frac{1}{2} \left(\frac{d^2\mu}{dx^2}\right)_{x=o} x^2 + \dots$$

[We will use this relation in the next section]

The transition dipole moment operator changes also as bond length changes with  $\hat{\mu} = q \hat{x}$ , where is the position operator  $\hat{x}$ . Since ' $\hat{x} = x \times$ ' (where  $\times$  is the multiplication sign) then  $\hat{\mu} = qx$ : the dipole moment operator is dependent on both the charge and the difference in distance between the charges, i.e. the atoms in the bond, compared to the equilibrium bond length.

Permanent dipole moments and especially the strength of the dipole moment are often related directly to the strength of electronic and vibrational (IR) absorption bands. However, it is the change in dipole moment during the excitation (absorption of a quantum of energy) that determines absorptivity rather than the strength of the permanent dipole moment.

#### 3.2. Transition dipole moments

Absorbing the energy of a photon results in a change in energy of a system (molecule) and, by definition, means a change in state, specifically from the initial state  $(\psi_i)$  to the final state  $(\psi_f)$  and this can either proceed directly (i.e. as in IR absorption spectroscopy) or via intermediate states (as we will see with Raman spectroscopy). In both cases, the transition involves the loss or gain of energy and angular moment through interaction of matter with photons. Unlike in the macroscopic world, the transition between the two states does not proceeds as a continuous process involves the mixing of states; there needs to be some mechanism (an operator) that describes the change (mixing) from the initial to the final state. In the quantum mechanical approach, the transition is achieved through an operator called the 'transition dipole moment' operator ( $\hat{\mu}$ ). Its name suggests the concept of dipoles changing during the change in state and for good reason. The change in dipole moment that is accompanies energy loss or gain by a molecule is quantified as  $\mu_f$ , the transition dipole moment. It is the change in dipole moment that occurs during the transition from the initial state ( $\psi_f$ ) to the final state ( $\psi_f$ ), i.e. the change in charge distribution.

Of course a change in state (energy) of a molecule can mean a change in the electronic, vibrational and rotational energy. However, because electron motion, and nuclear motion, and molecular rotation occur at different time scales (frequencies), then we can separate the total wavefunctions that describe each state into three parts:

$$\mu_{fi} = \int \psi_f^{\ \ \hat{i}} \hat{\mu} \psi_i d\tau = \int \left( \varphi_{e_i} \varphi_{v_i} Y_{J_i} \right)^{\hat{i}} \hat{\mu} \varphi_{e_i} \varphi_{v_i} Y_{J_i} d\tau$$

electronic  $(\varphi \dot{\iota} \dot{\iota} e)\dot{\iota}$ , vibrational  $(\varphi \dot{\iota} \dot{\iota} v)\dot{\iota}$  and rotational  $(Y \dot{\iota} \dot{\iota} j)\dot{\iota}$ . We can assume that the electronic and rotational states do not change during a vibrational excitation and since we consider only one axis (x), the equation simplifies to:

$$\mu_{fi} = \int \varphi_{v_f}^{\ i} \hat{\mu} \varphi_{v_i} dx$$

The transition dipole moment operator  $(\hat{\mu})$  reflects the redistribution of charge that occurs during the transition position (distance from the equilibrium bond length, see previous section).

We can replace  $\hat{\mu}$  and then separate out the terms.

$$\mu_{fi} = \int \varphi_{v_f}^{i} \left( \mu_o + \left( \frac{d \mu}{dx} \right)_{x=o} x + \frac{1}{2} \left( \frac{d^2 \mu}{dx^2} \right)_{x=o} x^2 + \dots \right) \varphi_{v_i} dx = \int \varphi_{v_f}^{i} \left( \mu_o \right) \varphi_{v_i} dx + \int \varphi_{v_f}^{i} \left( \left( \frac{d \mu}{dx} \right)_{x=o} x \right) \varphi_{v_i} dx + \int \varphi_{v_f}^{i} \left( \frac{1}{2} \left( \frac{d^2 \mu}{dx^2} \right)_{x=o} x \right) \varphi_{v_i} dx + \int \varphi_{v_f}^{i} \left( \frac{d \mu}{dx} \right)_{x=o} x \right) \varphi_{v_i} dx + \int \varphi_{v_f}^{i} \left( \frac{d \mu}{dx} \right)_{x=o} x + \frac{1}{2} \left( \frac{d^2 \mu}{dx^2} \right$$

The first two terms in the equation need only be considered as third and higher terms are minor under normal conditions and can be disregarded:

- The first term  $\mu_o \int \varphi_{v_f}^{\ \ \ \ \ } \varphi_{v_i} dx$  is only non-zero if the initial and final states are the same, if the states are different then  $\int \varphi_{v_f}^{\ \ \ \ \ } \varphi_{v_i} dx = 0$ . Remember that the vibrational states are orthogonal.
- The second term  $\left(\frac{d\,\mu}{dx}\right)_{x=0}\int \varphi_{v_f}^{\;\;\iota}(x)\varphi_{v_i}dx$  is zero also unless there is a change in dipole moment along the x-axis during the transition (Figure 6). Specifically the rate of change of dipole moment at x=0 must not be zero  $\left(\left(\frac{d\,\mu}{dx}\right)_{x=0}\neq 0\right)$ . Further analysis below (8.3.4) shows that the selection rule is  $\Delta v = +/-1$  which we will discuss when we consider the meaning of  $\int \varphi_{v_i}^{\;\;\iota}(x)\varphi_{v_i}dx$ .

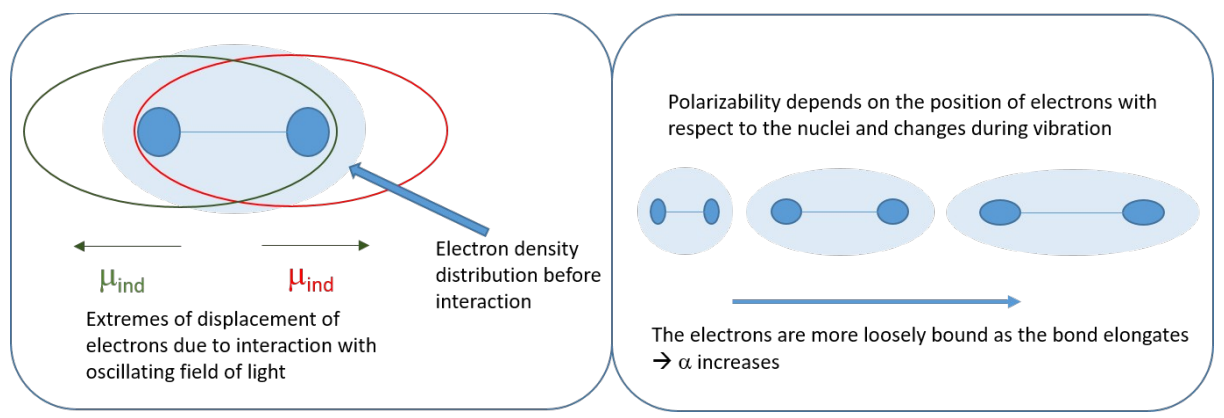


Figure 6. Variation of dipole moment with bond length.

#### 3.3. Polarizability, induced dipole moments, and scattering

The extent to which a material can respond to an oscillating electric field is expressed by a frequency dependent property, polarizability ( $\alpha$ ). In the context of Raman spectroscopy,  $\alpha$  is the ease with which the electron cloud can be disturbed by an electric field. An oscillating electric field (i.e. electromagnetic radiation) induces an oscillation in the position of the electrons in a molecule, which creates a transient (induced) dipole moment ( $\mu_{ind}$ ). The transient induced dipole moment differs from the permanent (static) dipole moment due to its time dependence;  $\mu_{ind}$  changes continuously. The light induced movement of electrons away from their equilibrium positions raises the energy of the molecule by the energy of the photon (hv) and the molecule is transiently excited to a higher energy state, referred to as a virtual state. We shall return to the concept of the virtual state later.

The strength of the induced dipole moment depends on how easily the electron cloud can be distorted and is directly proportional to the strength of the electric field  $(\vec{\mu}_{ind} \propto \vec{E}_t)$ . The polarizability is dependent on bond length, and hence on the nuclear coordinates  $(Q_{ij})$ , and varies over an oscillation (vibration), Figure 7; increasing as the nuclei move further apart and decreasing as the nuclei approach each other. However, the polarisation induced depends also on the bond length and the constant of proportionality varies with bond length,  $\mu_{ind} = \alpha_x \vec{E}_t$ . This dependence opens a potential mechanism to induce a change in state in a molecule as described by the induced dipole moment operator,  $\hat{\mu}_{ind} = \alpha_x \vec{E}_t$ .

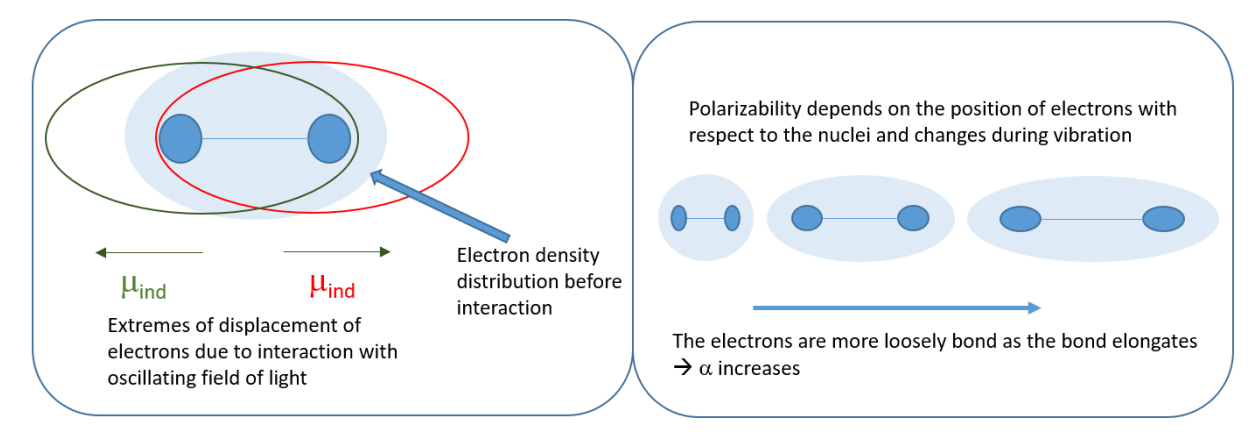


Figure 7 An electric field oscillating in the  $10^{15}$  Hz range will induce a transient dipole moment by moving the electrons in a molecule. The ease with which this can occur depends on the difference in bond length compared to the equilibrium bond length – when elongated the electrons are more loosely bound and are easier to displace and vice-versa.

The magnitude of  $\alpha_x$  can be defined with reference to the polarizability when the nuclei are at their equilibrium positions (x = 0). If we look again at the equation derived above for the transition dipole moment (8.3.2.) but this time consider the induced dipole moment rather than a permanent dipole moment, then we can substitute  $\hat{\mu}_{ind}$  with  $\alpha_x \vec{E}_t$  the equation:

$$(\mu_{ind})_{fi} = \int \varphi_{v_i}^{\ \ \iota} \hat{\mu}_{ind} \varphi_{v_i} dx = \int \varphi_{v_i}^{\ \ \iota} (\alpha_x \vec{E}_t) \varphi_{v_i} dx = \vec{E}_t \int \varphi_{v_i}^{\ \ \iota} (\alpha_x) \varphi_{v_i} dx$$

The polarizability depends on position (distance from the minimum) since as the nuclei move further apart or closer together their electrostatic interaction with the electrons changes. We can calculate  $\alpha_x$  using a Taylor expansion:

$$\alpha_x = \alpha_o + \left(\frac{d\alpha}{dx}\right)_{x=o} x + \frac{1}{2} \left(\frac{d^2\alpha}{dx^2}\right)_{x=o} x^2 + \dots$$

Since the bond length changes little during a vibration and the 3<sup>rd</sup> (hyperpolarizability), and higher terms are essentially zero, we need only consider the first two terms:

$$(\mu_{ind})_{fi} = \vec{E}_t \int \varphi_{v_f}^{\ \ \iota}(\alpha_x) \varphi_{v_i} dx = \vec{E}_t \int \varphi_{v_f}^{\ \ \iota} \left(\alpha_o + \left(\frac{d\alpha}{dx}\right)_{x=o} x\right) \varphi_{v_i} dx = \vec{E}_t \int \varphi_{v_f}^{\ \ \iota}(\alpha_0) \varphi_{v_i} dx + \vec{E}_t \int \varphi_{v_f}^{\ \ \iota} \left(\left(\frac{d\alpha}{dx}\right)_{x=o} x\right) \varphi_{v_i} dx = \alpha_0$$

The first term  $\alpha_0 \vec{E}_t \int \varphi_{v_i}^{\ \ \ } \varphi_{v_i} dx$  is zero unless the initial and final states are the same, i.e. if  $\int \varphi_{v_i}^{\ \ \ \ \ } \varphi_{v_i} dx = 0 \text{if } \varphi_{v_i} \neq \varphi_{v_i}$  and  $\int \varphi_{v_i}^{\ \ \ \ \ \ \ } \varphi_{v_i} dx = 1 \text{if } \varphi_{v_i} \vec{c} \varphi_{v_i}.$ 

Hence, if the initial and final states are the same then the induced transition dipole moment is large, which is consistent with the intensity of Rayleigh scattering compared with Raman (Stokes and anti-Stokes) scattering.

For Raman scattering to take place then the initial and final states cannot be the same and therefore the first term is zero and the second term has to be non-zero. The second term is non-zero if the initial and final states differ by one quantum (i.e.  $\Delta v = +/-1$ , see the next section) and if the rate of change in polarizability at the minimum of the potential well is non-zero, i.e.,  $\left(\frac{d\alpha}{dx}\right)_{x=o} \neq 0$ . Hence the polarizability has to change during the oscillation.

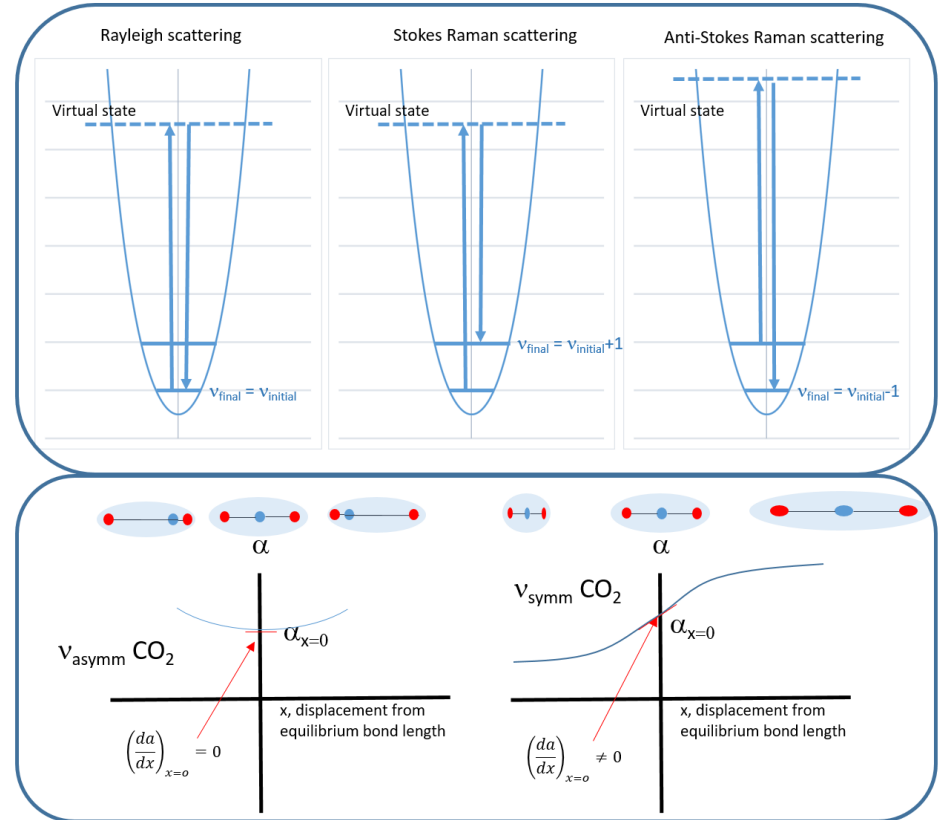


Figure 8. Rayleigh, Stokes, and anti-Stokes Raman scattering, note in the case of anti-Stokes Raman scattering the virtual state (see section 8.3.6) reached is different, but the gap between the initial and virtual states is the same as for Stokes and Rayleigh scattering. The Raman process is allowed only if the rate of change in polarizability at the equilibrium bond length is not zero  $\left(\frac{d\alpha}{dx}\right)_{x=0} \neq 0$ .

### 3.4. What is $\int \varphi_{v_i}^{\ \ i}(x)\varphi_{v_i}dx$ ?

The wavefunctions for vibrational states are based on a, the Hermite polynomials, which are a set of orthogonal functions weighted by the Gaussian function  $\left(e^{-z^2}\right)$ , that satisfy the boundary conditions for oscillation in a potential well (so called eigenstates). Their precise description can be found elsewhere, but a brief discussion is warranted here to explain the gross selection rule for Raman and IR spectroscopy and rationalise the origin of Rayleigh scattering, and Stokes and anti-Stokes Raman scattering.

In the following:

• 
$$a = \left(\frac{\hbar^2}{m_{eff} k_f}\right)^{\frac{1}{4}}$$

- $N_{v_i}$  and  $N_{v_f}$  are normalisation constants with  $N_v = \left(\frac{1}{\alpha \sqrt{\pi} \, 2^v v!}\right)^{\frac{1}{2}}$
- $H_{\nu}$  is a Hermite polynomial for a vibrational level (Figure 4).
- $y = \frac{x}{a}$
- The wavefunctions  $\varphi_v$  are Gaussian ( $e^{\frac{-y^2}{2}}$ ) modified by the Hermite polynomial  $H_v$ :  $\varphi_v = H_v e^{\frac{-y^2}{2}}$ .

The  $2^{nd}$  term above can be expanded on using the Hermite polynomials corresponding to each level; in this case .

$$\int \varphi_{v_f}^{\ \ c}(x)\varphi_{v_i}dx = N_{v_f}N_{v_i}\int_{-\infty}^{\infty} \left(H_{v_f}e^{\frac{-y^2}{2}}\right)y\left(H_{v_i}e^{\frac{-y^2}{2}}\right)dx = N_{v_f}N_{v_i}\int_{-\infty}^{\infty}H_{v_f}yH_{v_i}e^{-y^2}dx = a^2N_{v_f}N_{v_i}\int_{-\infty}^{\infty}H_{v_f}yH_{v_i}e^{-y^2}dy$$

We make use of the recurrence relation:  $y H_v = v H_{v-1} + \frac{1}{2} H_{v+1}$  to obtain (Figure 8):

$$\int \varphi_{v_{i}}^{i}(x)\varphi_{v_{i}}dx = a^{2}N_{v_{i}}N_{v_{i}}\int_{-\infty}^{\infty}H_{v_{i}}\left(vH_{v_{i}-1} + \frac{1}{2}H_{v_{i}+1}\right)e^{-y^{2}}dy = a^{2}N_{v_{i}}N_{v_{i}}\left[v_{i}\int_{-\infty}^{\infty}H_{v_{i}}yH_{v_{i}-1}e^{-y^{2}}dy + \frac{1}{2}\int_{-\infty}^{\infty}H_{v_{i}}yH_{v_{i}+1}e^{-y^{2}}dy\right]$$

- The first term  $\int_{-\infty}^{\infty} H_{v_f} y H_{v_{i-1}} e^{-y^2} dy$  describes anti-Stokes Raman scattering and is zero unless  $v_f = v_{i-1}$
- The second term  $\frac{1}{2} \int_{-\infty}^{\infty} H_{\nu_i} y H_{\nu_i+1} e^{-y^2} dy$  describes Stokes Raman scattering and is zero unless  $v_f = v_{i+1}$

In summary, only transitions from  $v_i$  to  $v_{i+1}$  and from  $v_i$  to  $v_{i-1}$  are allowed and hence we have the selection rule  $\Delta v = \pm 1$ . In all other circumstances the integrals evaluate as zero and hence overtones are forbidden in Raman spectroscopy, except under specific circumstances (see below).

It should be noted that for a harmonic oscillator the separation between each vibrational level is constant, however, in molecules the spacing between the energy levels decreases with increasing vibrational level number due to anharmonicity. Hence, although the probability of transitions where  $\Delta v \neq \pm 1$  should be zero, the anharmonicity provides some allowedness for direct excitation by a resonant photon, i.e. infrared absorption, in addition to the fundamental transition between the 0<sup>th</sup> and 1<sup>st</sup>, transitions between the 0<sup>th</sup> and 2<sup>nd</sup> (1<sup>st</sup> overtone) and 0<sup>th</sup> and 3<sup>rd</sup> (2<sup>nd</sup> overtone) vibrational levels can occur, but with an order of magnitude decrease in molar absorptivity with each additional step.

As a final remark in this section, in addition to fundamental transitions, other terms that appear frequently in a discussion of vibrational spectroscopy are:

**Normal modes.** This term appears frequently in the discussion of vibrational spectra. A normal mode is an independent synchronous motion of atoms for which excitation does not lead to excitation of other modes and does not lead to translation or rotation of the molecule.

**Overtones:**  $(v_2 \leftarrow v_0, v_3 \leftarrow v_0 ... etc. \dot{c}$  are transitions where  $\Delta v \neq \pm 1$  and are formally forbidden. **Combination bands** are bands due to the excitation of two normal modes simultaneously, in and out of phase.

#### 3.5. Relative intensities of Stokes and anti-Stokes Raman scattering

The ratio of the Stokes and anti-Stokes scattering depends primarily on the relative number of molecules that are in the lowest or first vibrational state under the conditions used, and is governed by the Boltzmann distribution:

$$\frac{N_i}{N_i} = \frac{g_i}{g_i} e^{\left(\frac{-\Delta E}{k_B T}\right)}$$

where N the number of molecules in the lower and upper vibrational states, g is the degeneracy of the states, and  $\Delta E$  is the energy gap between the vibrational states. The number of molecules that are in vibrational states above the lowest vibrational state is dependent on temperature. At room temperature about 200 cm<sup>-1</sup> energy is available. The larger the gap or in other words, the higher the wavenumber or frequency of a mode, the less likely that molecules will be present in the 1<sup>st</sup> or 2<sup>nd</sup> vibrationally excited state and hence in the anti-Stokes Raman spectrum the lowest wavenumber bands are generally the most intense.

#### 3.6. What is a virtual state?

Raman spectra recorded where the wavelength of excitation is much longer (lower energy) than the lowest electronic transition are referred to as non-resonant. Under these conditions the interaction of electromagnetic radiation (i.e. the oscillating electric field) with the electrons in molecules results in displacement from their lowest energy arrangement. This displacement occurs on a time scale much shorter than required for the nuclei to respond and move. The change in energy is represented as a vertical transition in the normal coordinate diagram shown below. The name 'virtual state' reflects the fact that although the nuclei are still at the same position as they were before interaction with the electric field, the electrons are now disturbed from their stable distribution and as a result the energy of the molecule has increased by the same energy as the photon contained. Hence, the 'virtual' state is real but does not represent a true electronically excited (or formally a stationary) state and the wave packet  $(\phi)$  has the same initial 'shape' as that of the ground vibrational state (the Franck Condon principle, Figure 9a). The term 'Frank Condon factors' appears frequently in the discussion of vibrational and electronic spectroscopy and it is worth taking a moment to consider its meaning (Figure 9b). Using the Born Oppenheimer approximation, the nuclei are static on the time scale that electrons move then for a transition to take place the overlap of the wavefunctions of the initial and final vibrational states (i.e. the distribution of the nuclei) has to be non-zero:  $\int \varphi_{v_i}^{\ \ \ } \varphi_{v_i} dx \neq 0$ .

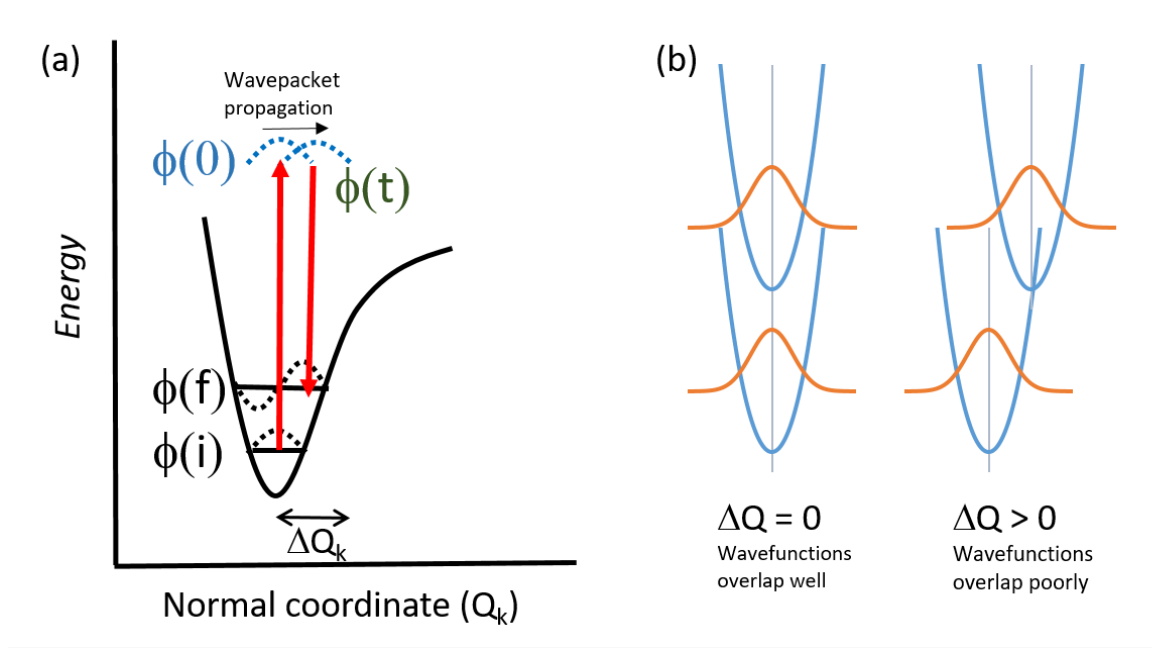


Figure 9. (a) Illustration of excitation to a virtual state 'wavepacket' ( $\phi$  blue dotted line), which relaxes back to ( $\phi$ (i)) before propagation of the wavepacket ( $\phi$ (t), movement of nuclei) creates a

significant non-zero Frank Condon overlap with a vibrational state ( $\phi(f)$ ) other than the initial vibrational state ( $\phi(i)$ ). (b) Example of high and low overlap of wavefunctions and hence high and low overlap integrals (Franck Condon factors).

We will see, later in our discussion of the description of the Raman effect proposed by Heller, that the nuclei begin to move immediately (wavepacket propagation,  $\phi(t)$ ). The movement (displacement) is limited as the electrons return to their original distribution ( $\chi(i)$ ) by generation of a photon of the same frequency as the incident photon (Rayleigh scattering) before significant changes in nuclear position (compared to  $\phi(i)$ ) can take place. Occasionally, and with a probability of the order of 1 in 10-100 million, the wavepacket will have propagated sufficiently (i.e. nuclei actually move slightly) that relaxation to a different vibrational level ( $\phi(f)$ ) of the ground state will occur, since the overlap integral (between the two vibrational wavefunctions in the virtual and ground states) is no longer zero, giving rise to Stokes or anti-Stokes Raman scattering.

#### 4. The (resonance) Raman experiment

From an experimental perspective, Raman spectroscopy is relatively straightforward. A laser is focused onto a sample and some of the light scattered is collected by lenses, focused into a spectrograph and dispersed on a CCD (Charge Coupled Device) array to generate a spectrum of intensity of scattered light vs. wavenumber shift (Figure 10a). The vast majority of the light scattered is the same wavelength as that of the laser and will swamp the weak Raman shifted scattering if it enters the spectrograph. Hence a steep long pass filter is used to allow only light of longer wavelength (or shorter wavelength in the case of anti-Stokes Raman spectroscopy) than the laser wavelength to enter into the spectrograph.

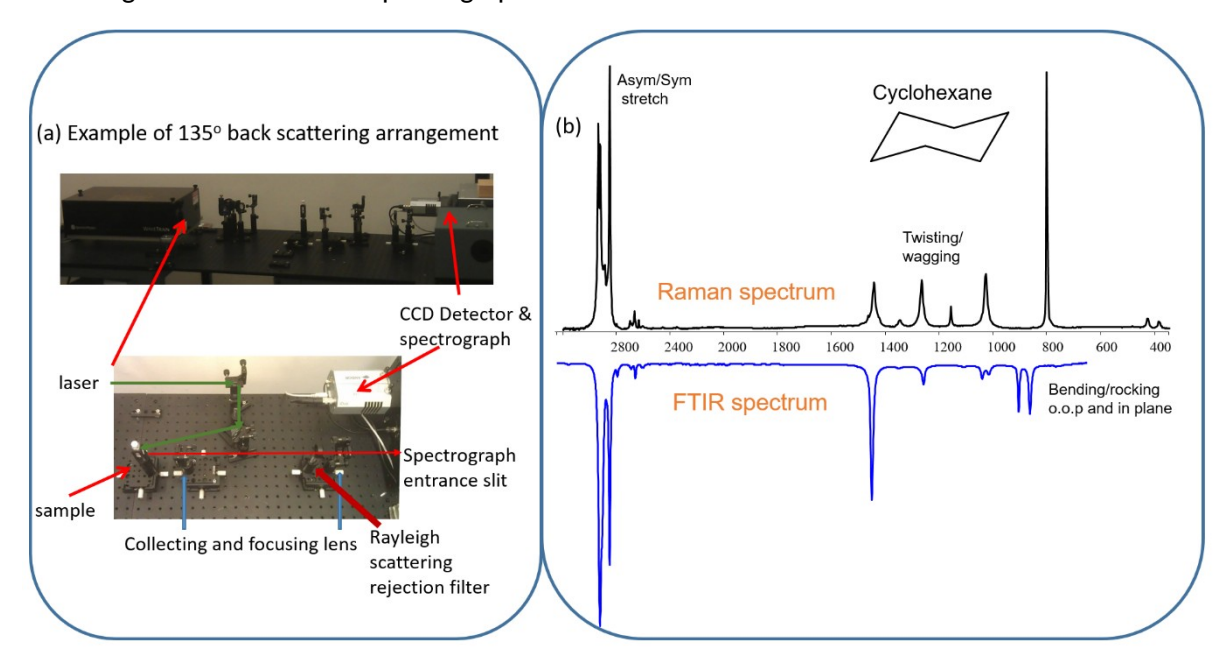


Figure 10. (a) A basic experimental arrangement for Raman spectroscopy. (b) Comparison of Raman and FTIR spectra of cyclohexane.

The Raman spectrum generated is analogous to an FTIR spectrum with the key difference that the selection rules and hence relative intensity of bands are different (Figure 10b). However, the expected positions for particular bands in FTIR spectroscopy are the same in Raman spectroscopy, and tables of expected band positions for IR spectroscopy are equally applicable in the interpretation of Raman spectra.

An important technical difference, however, is that although Raman spectra are reported with the abscissa in wavenumbers (cm<sup>-1</sup>), corresponding to the far and mid-infrared parts of the electromagnetic spectrum, the photons (light) that are received by the detector in Raman spectroscopy are in fact in the visible or near infrared region. Indeed the abscissa in Raman spectra should be labelled as Raman shift ( $\Delta$ cm<sup>-1</sup>), where  $\Delta$  refers to the difference in energy between the excitation laser and the Raman scattering, as illustrated in figure 11.

Furthermore, the laser used to record Raman spectra must have a narrow spectral linewidth; that is to say that the emission spectrum of the laser must have a full width at half maximum (FWHM) that is much less than the natural linewidth of the Raman bands (i.e. < 0.3 cm<sup>-1</sup>, or 1 GHz).

As with IR spectroscopy, the Raman spectrum is a manifestation of the both the shape (nuclear coordinates) and distribution of electron density of the molecule. Symmetry and group theory are therefore key mathematical tools in the prediction and interpretation of spectra, a discussion of which is beyond the scope of this chapter. An example of the importance of symmetry (molecular shape) to the appearance of vibrational spectra is shown in Figure 12. The well-known ligand 2,2'-bipyridine adopts a conformation in which the nitrogen atoms are trans to each another to reduce steric hindrance between the H5/H5' hydrogens. When bound to a metal ion, the structure is reversed and while the spectrum is similar, in the sense that bands are present in the same regions of each spectrum, the positions and relative intensity of the bands are different, reflecting the change in shape.

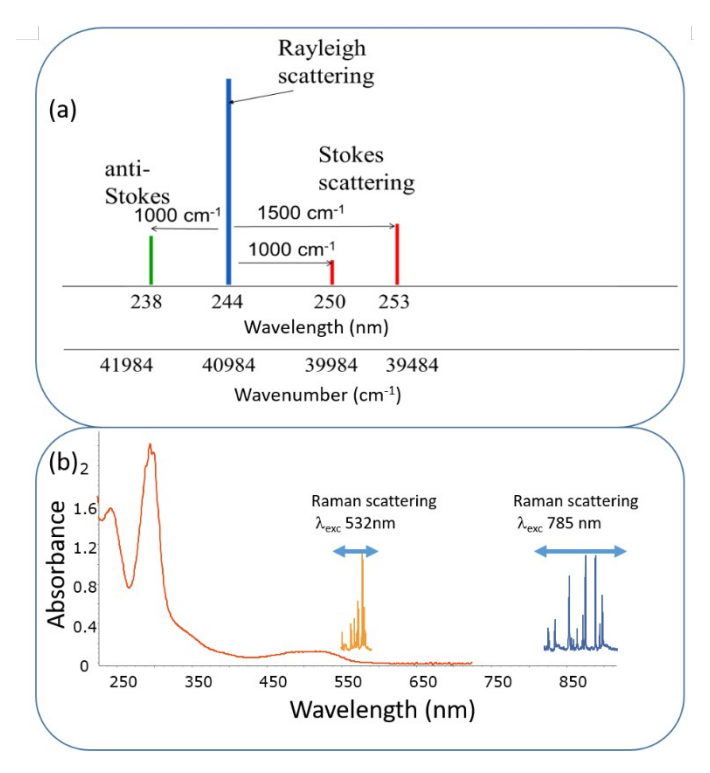


Figure 11. (a) Relation between laser wavelength and wavelength of photons responsible for Stokes and anti-Stokes Raman scattering. Note that the Raman shift is the difference in wavenumbers between the excitation laser and the wavelengths of the Raman photons. (b) UV/Vis absorption spectrum of  $[Fe(bipy)_3]^{2+}$  (ca. 0.1 mM) overlaid with Raman spectra recorded at 532 nm and 785 nm (ca. 0.5 M) showing the energy of the Raman photons in nm rather than the more usual wavenumber shift. Note that the Raman scattering at 532 nm overlaps with an absorption band of the complex but that at 785 nm does not (see section 8.7.3).

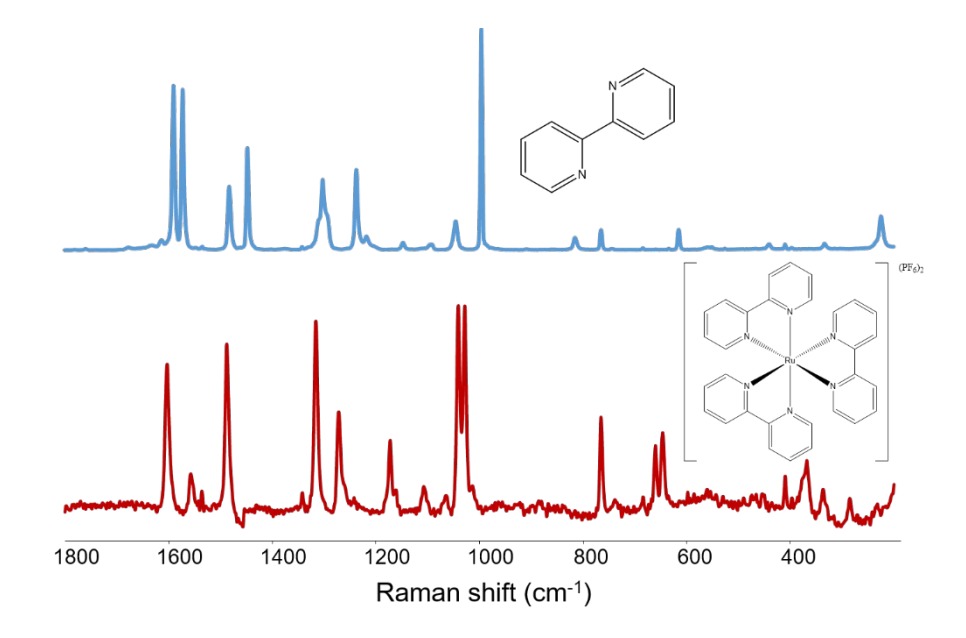


Figure 12. Raman spectra ( $\lambda_{exc}$  785 nm) of solid samples of 2,2'-bipyridine and its ruthenium(II) complex  $[Ru(bipy)_3]^{2+}$ .

#### 4.1. Raman cross-section and the intensity of Raman bands

There are two aspects of vibrational spectroscopy with which we are concerned; band position and band intensity. In both IR and Raman spectroscopy, the band position (resonant frequency) is dependent on the strength of the bond  $(k_f)$  and the effective mass of the oscillators. In IR spectroscopy, transmittance is dependent non-linearly on concentration and the transmission pathlength and hence for quantitative work absorbance and molar absorptivity are used. Since we use the ratio of light transmitted with and without the sample we give little, if any, thought usually to instrumental aspects (intensity of the lamp, detector response, etc.). In contrast, band intensity in Raman spectroscopy is dependent on a number of factors including practical/physical parameters such as the intensity of excitation light (laser,  $I_{\rm exc}$ ), the frequency of the laser (v), the solid angle  $(\Omega)$  over which the Raman scattering is collected, concentration (number of molecules in the confocal volume, N), and the square of the rate of change of polarizability  $(\alpha)$  at the equilibrium nuclear coordinates (Q):

Intensity 
$$\propto v^4 I_{exc} \Omega N \left( \frac{\partial \alpha}{\partial Q} \right)^2$$

From an experimental perspective, the first four terms  ${}'v^4I_{exc}\Omega N$  are of practical importance and responsible for the increase in Raman intensity at shorter wavelengths. All things being equal, with regard to detector sensitivity, the same intensity can be achieved at 266 nm using a laser power of ca. 1.2 mW as at 785 nm with 100 mW, or at 1064 nm with 300 mW.

Table 1 Dependence of Raman scattering on laser wavelength.

Wavelength	
(nm)	Raman intensity relative to 1064 nm
266	256
355	81
532	16
632.8	8

785 3 1064 1

However, detector sensitivity and the performance of optics and gratings can have a large influence on the overall intensity and hence the increase in Raman scattering is not a major consideration in choice of wavelength of laser. From a practical perspective the intensity of a Raman band scales linearly with concentration (Figure 13) and the solvent itself, or another compound can act as an internal reference to correct for variations in other parameters between measurements.

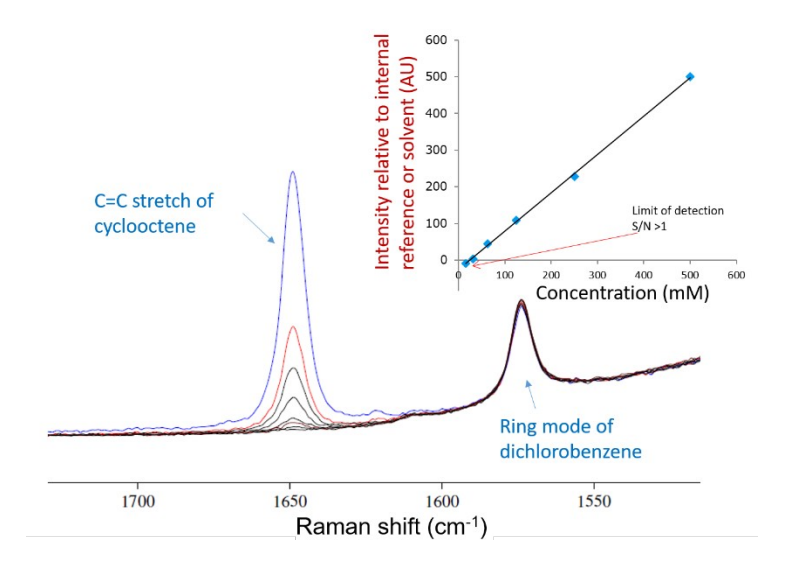


Figure 13. Variation in Raman ( $\lambda_{\rm exc}$  785 nm) band intensity with concentration for cyclooctene in CH<sub>3</sub>CN with 1,2-dichlorobenzene as internal reference. Inset: calibration curve generated from data showing linearity and limit of detection.

#### 4.2 Raman scattering is a weak effect; but how weak?

As a point of reference, high performance Raman spectrometers can expect to achieve limits of detection between 10 to 100 mM. However, this is dependent on the nature of the analyte and its polarizability and in our own experience the limit of detection for non-resonant Raman scattering can be as low as 5 mM, but for compounds such as  $H_2O_2$ , even under ideal situations the limit is at best 20 mM, and more usually 100 mM. In contrast, in many biological systems the concentration of the chromophore of the species under examination can be as low as in the low micromolar concentration range. These concentrations pose a challenge to the limits of detection of many techniques, not least Raman spectroscopy.

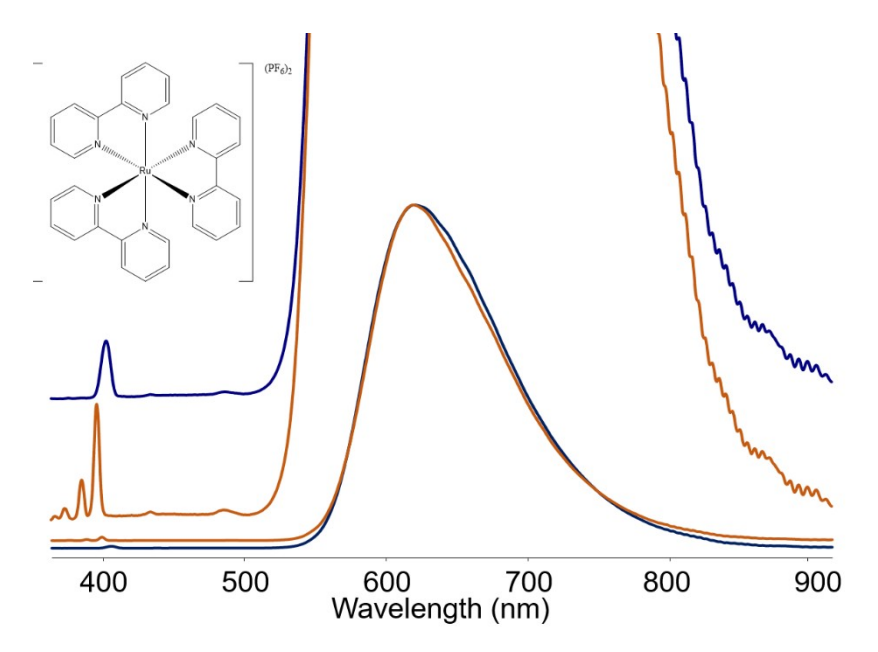


Figure 14. Comparison of the intensity of the emission from the complex  $[Ru(bipy)_3]^{2+}$  (10  $\mu$ M) in water (blue) and acetonitrile (orange) with the Raman scattering from the solvent with excitation at 355 nm (10 mW). The spectra are expanded to reveal the Raman scattering between 350 and 410 nm.

A feeling for how weak the Raman effect is can be gained by considering Figure 14. The emission spectrum of the well-known luminophore [Ru(bipy)<sub>3</sub>]<sup>2+</sup> in water and acetonitrile is shown with excitation at 355 nm in this particular case. The emission spectrum, in terms of shape, does not depend on excitation wavelength and hence by choosing 355 nm we can easily see the Raman scattering from the solvent also. This demonstrates that the only difference between a spectrofluorimeter and a Raman spectrometer is performance (i.e. narrow linewidth laser and high resolution spectrograph). However, it should be noted that the emission spectra have been scaled by several orders of magnitude, so that the Raman scattering is noticeable. If we note that the transmission is 90% at 355 nm and therefore [Ru(bipy)<sub>3</sub>]<sup>2+</sup> absorbs 10% of the 10 mW of light impinging on it and reemits at most 0.02% of that light, then the total area of the emission spectrum represents 2  $\mu$ W or 1 in 5000 photons. The area of the Raman scattering is ca. 0.01% of the area of the total emission and hence only 1 in 50 million of the photons hitting the sample are scattered as Raman scattering! Furthermore, the concentration of most analytes of interest are typically in the 10 to 100 mM range and hence we reach the 1 in 25 billion photons range. This of course is a 'back of the envelope' calculation and is therefore imprecise, however, it serves to highlight the challenge faced in recording Raman spectra. It should also be noted that, in this example, the wavelength of the laser used was chosen so that the Raman scattering would appear in a region of the spectrum where it does not overlap with the emission spectrum of the complex. If the laser used was at 532 nm, in principle, the narrow Raman bands would sit 'on top' of the very broad emission band and a simple baseline correction could be applied to see only the Raman spectrum. However, this will not work due to 'shot noise'. Shot noise is the major source of noise with CCD cameras used in Raman systems and the noise (N) scales with the total intensity (Shot noise  $\propto \sqrt{Signal}$ ) and hence the noise is due to the total signal (Emission + Raman scattering) and not just the Raman scattering. In short, fluorescence/phosphorescence present in the wavelength range where Raman scattering is generated will often swamp the weak Raman signal and make it essentially impossible to record a useful spectrum. With non-resonant Raman the solution is of course to use a different laser

wavelength, however, for resonance Raman spectroscopy, which is the subject of this chapter, this can mean 'moving out of resonance'.

#### 5. Resonance enhancement of Raman scattering

In the study of bioinorganic systems, a major challenge is that of the intrinsically low concentration of the species under examination, for example a metalloenzyme. Indeed, even in its pure form the weight percentage of the active site within the protein is often relatively low. Hence, it is not obvious that Raman spectroscopy, a phenomenon that is improbable and with detection limits typically in the 10 to 100 mM range, would become a leading technique in the field. The success of Raman spectroscopy lies in the effect referred to as resonance enhancement, in which the Raman scattering by a chromophore can be enhanced by orders of magnitude and resulting in limits of detection for such a species as low as the micromolar range. In this section the phenomenon of resonance enhancement and the technique known as **Resonance Raman spectroscopy** will be discussed. However, we will start with a simple but essential point:

There is no such thing as a resonance Raman spectrometer; and there is no such thing as running a resonance Raman spectrum.

The experiment, referred colloquially as resonance Raman spectroscopy, is in all cases with all samples simply the recording of a Raman spectrum on a standard spectrometer equipped with a laser that is chosen to be 'resonant' with, has the same wavelength as, an optical absorption band of the chromophore of interest.

#### 5.1. The Raman spectroscopy of carrots and parrots

We will first consider the expected Raman spectrum of a carrot to illustrate the effect of resonance enhancement. The Raman spectrum of a root vegetable, for example a parsnip or a carrot, would be expected to be composed of scattering due to the major components primarily, in order of concentration, water, polysaccharides (sugars), lipids, and proteins. Trace components i.e. those with concentrations less than 10 mM, will not contribute significantly as the Raman scattering they produce is likely to be below the signal to noise threshold. Water and carbohydrates are by far the major components but generally give weak Raman scattering and we would expect bands due to water stretching and bending at ca. 3500 and 1600 cm $^{-1}$ . In addition bands at just below 3000 cm $^{-1}$  due to aliphatic C-H stretching and at 1400 and 1250 cm $^{-1}$  due to C-H wagging and C-C stretching modes. Bands at essentially the same positions will be observed for lipids and proteins present in addition to weak contributions from esters and amides. The spectrum of a carrot recorded with a laser at 632.8 nm is shown below. The spectrum is far from that expected (Figure 15). Two intense bands are present, at 1250 and 1550 cm $^{-1}$  that are consistent with a polyene ( $\beta$ -carotene) rather than any of the expected contributions from lipids and carbohydrates. The dominance of these bands are due to resonance enhancement.

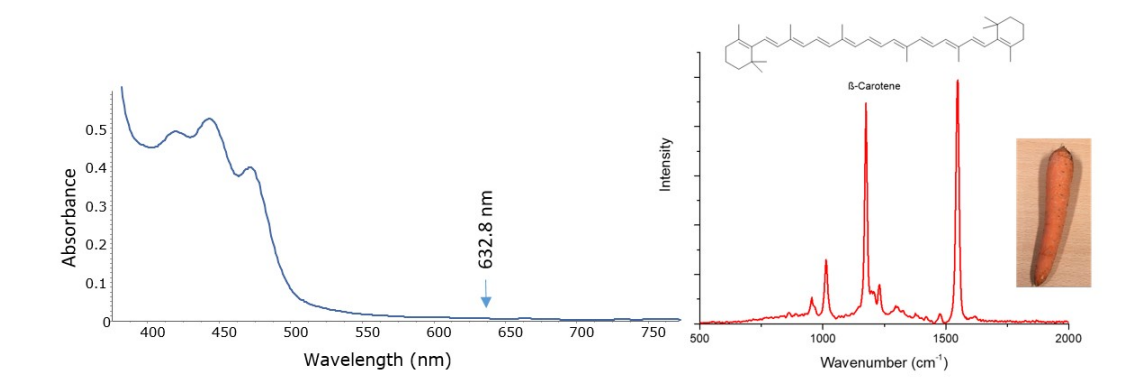


Figure 15. UV/vis absorption spectrum (of ethanol extract) of a carrot and Raman spectrum of untreated carrot ( $\lambda_{\rm exc}$  632.8 nm). Although the wavelength of the laser is 150 nm longer than the lowest absorption band of the carrot, pre-resonance enhancement is substantial.

A more subtle example of resonance enhancement can be seen in the Raman spectra of parrot feathers. Colour is of substantial importance in the natural world, seen most vividly in the striking colour combinations presented by members of the parrot family. Colour can arise from either of two sources; structural and absorptive. In the case of structural colour, the space between layers of biomaterials or periodicity of liquid crystals are close to those of the wavelength of light and interference phenomena create colour or the Tyndall effect is employed, for example, to scatter blue light. These approaches are used especially to achieve iridescence and blue/green colours. Black is typically due to cross-linked polyphenolics (i.e. melanin produced from polymerisation of oxidised tyrosine). The red and yellow colours are typically produced by organic chromophores, however, their identity is difficult to determine, due their extremely low concentrations within the biological matrices they are contained in, and extraction methods can lead to reactions that alter chemical structure.

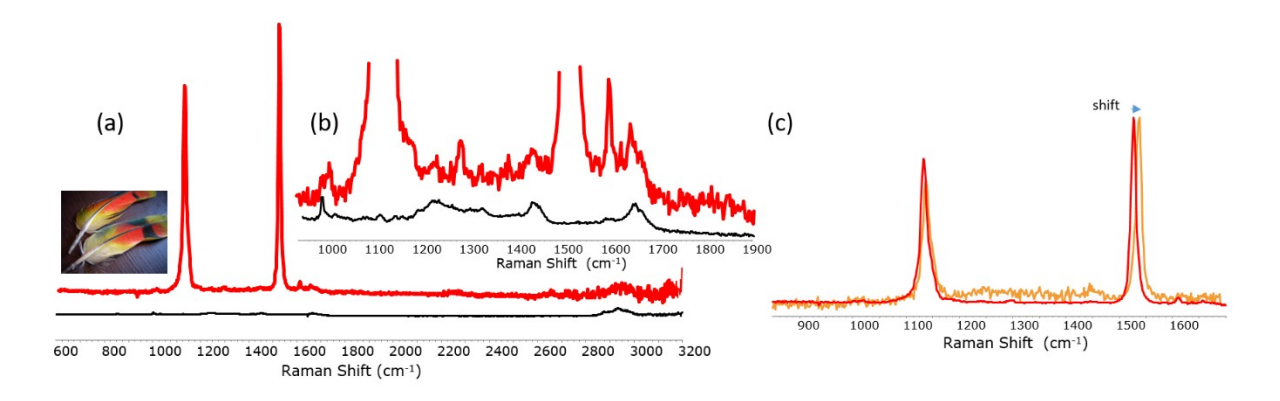


Figure 16. Raman spectra ( $\lambda_{\text{exc}}$  632.8 nm) of a white (black line) and red (red line) region of a feather from a Malukken Kakatoe (a) full scale and (b) expansion to show weak collagen bands. (c) Raman spectra of yellow (yellow spectrum) and red (red spectrum) regions showing the 6-10 cm<sup>-1</sup> shift in the main bands.

Taking a parrot feather as an example, we would predict a Raman spectrum based on the composition of the feather, which is essentially collagen and indeed when a white feather or the stalk is focused on with a red laser (e.g., 632.8 nm in this case) the spectrum, although weak, shows all expected bands of the amino acids present in collagen Figure 16. Focusing on a black region results in burning of feather due to heating caused by the absorption of the light and little

information can be extracted. By contrast if we examine a red or yellow region, we see the expected weak Raman scattering of the protein matrix, but also several very intense bands at ca. 1100 and 1550 cm<sup>-1</sup>. These bands are due to Raman scattering from the chromophore, which, although present in micromolar or lower concentrations, show strong Raman scattering. Comparison of the spectrum with that of the carrot above leads to the immediate conclusion that the chromophore is a carotenoid, however, the differences in wavenumber positions indicate that they are not identical structures. When the focus point is moved to a yellow region of the feather the general shape of the spectrum obtained is largely the same, however, there are two noticeable differences. The peak positions are shifted and the signal to noise ratio has decreased considerably. The latter effect is consistent with a difference in the absorption spectra of the chromophores with the compound providing the yellow colour absorbing less at 632.8 nm (the wavelength of the laser used in this case) and hence the resonance enhancement expected is less (there is an increase in the denominator in the Kramers Heisenberg Dirac (KHD) equation for polarizability, see below). The difference in wavenumber shift of the bands is not due to optical effects as in the region between yellow and red, it is clear that the spectrum is a sum of the two contributing spectra. The change in wavenumber indicates a change in structure but it must be remembered that this change can be due to conformational effects induced by a surrounding protein environment (as is the case with retinal), rather than a change in molecular structure. Remember that the vibrational spectrum reflects the structure in three dimensions and hence a change in conformation is sufficient to change the vibrational, as well as visible absorption, spectrum.

These examples, although somewhat trivial, highlight a number of important aspects of resonance Raman spectroscopy. Firstly, in all cases the spectrum is simply a Raman spectrum in terms of how it is recorded. The wavelength of the laser used has a large effect on the absolute intensity of the Raman scattering due to the  $1/\lambda^4$  dependence on Raman intensity on wavelength. If the laser is in resonance with an electronic transition in a compound, then the Raman scattering for that compound can be increased by many orders of magnitude. In this case, the Raman spectrum is dominated by the carotenes, despite that they are present in concentrations typically of 0.1 mg/g or 0.01%.

In the next section, we will consider the origin of this increase in intensity but first we will look at how the Raman scattering from the solvent and a coloured compound dissolved in it changes as the wavelength of the laser is changed from 785 nm to 244 nm. As the laser wavelength approaches the visible absorption bands, the Raman scattering from the compound is expected to increase substantially due to resonance enhancement. However, as we will see, this does not necessarily occur. The complex  $[Cu(dmbipy)(H_2O)_2]^{2+}$  absorbs strongly in the UV region  $(\pi\pi^*$  transitions) and only weakly in the visible and NIR region (metal centred absorption bands), Figure 17.

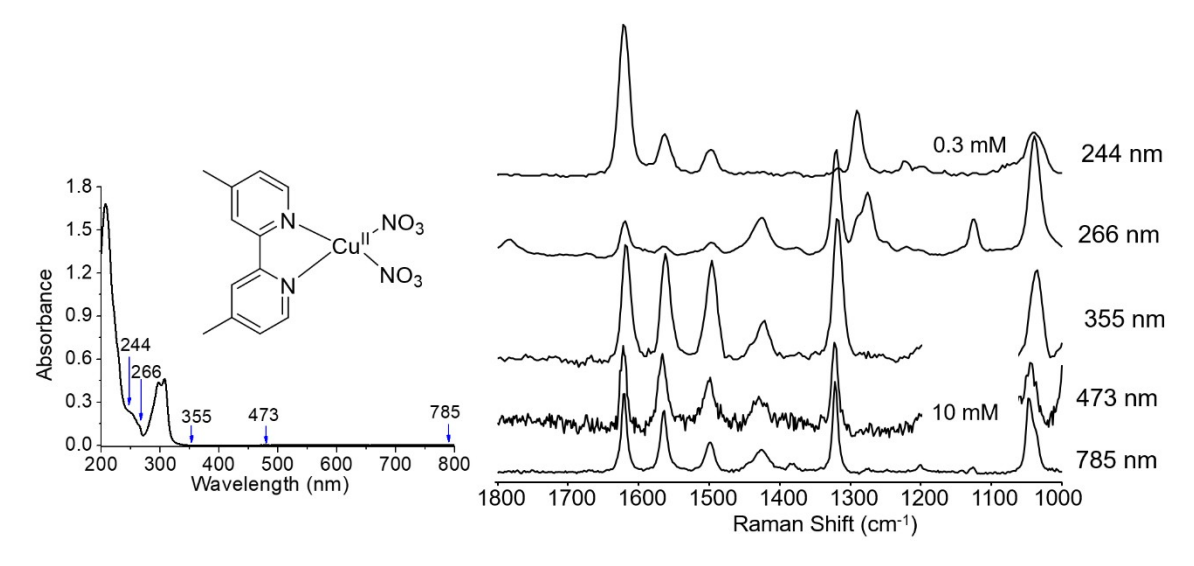


Figure 17. Raman spectrum of  $[Cu(dmbipy)(H_2O)_2]^{2+}$  at various non-resonant and resonant wavelengths (Draksharapu, Boersma, et al. 2015). The concentration used was 100 mM at 785 nm, 10 mM at 473 nm and 0.3 mM at all other wavelengths.

When we compare the spectra from which Raman scattering from the solvent have been removed by spectral subtraction, it becomes apparent that the band positions match exactly, i.e. the Raman bands appear with exactly the same wavenumber in spectra obtained both on and off resonance. However, as resonance enhancement becomes more pronounced it becomes clear that the relative intensity of bands, even those that are of similar wavenumber, varies dramatically. This is an important feature of resonance Raman spectroscopy and these differences in relative intensity of bands allows us to probe or to verify the electronic structure responsible for the absorption bands, and in particular to identify the type of transition it is (e.g. metal cantered, ligand to metal (LMCT) and metal to ligand (MLCT) charge transfer, etc.) and which parts of the molecule undergo changes in electron density as a result of the excitation. In summary, in addition to an overall increase in Raman scattering intensity the phenomenon of resonance enhancement is characterised by the observation that:

- the Raman scattering from only a limited number of modes undergo significant enhancement, i.e. not all bands observed in the Raman spectrum of a compound will be observed under conditions of resonance enhancement
- the relative intensity of bands will often be different at different resonance wavelengths
- the position (in wavenumber, cm<sup>-1</sup>) of the enhanced bands are identical to those observed in the Raman spectrum recorded under non-resonant conditions, i.e. at a wavelength far removed from an electronic absorption band of the compound.

#### 5.2 Classical description of Rayleigh and Raman scattering

There are a number of approaches that can be taken to explain the interaction of light with molecules (Long 1977). The classical approach makes use of the relation between polarization P and the strength of the electric field, which microscopically is expressed as  $\vec{\mu}_{ind} = \alpha \, \vec{E}_t$ . In the case of electromagnetic radiation  $\vec{E}_t = \vec{E}_0 \cos 2 \pi \, v_0 \, t$ , where  $\vec{E}_0$  is the amplitude of the oscillating electric field and  $v_0$  is the frequency of the electromagnetic radiation (in the visible region 10 <sup>15</sup>-10 <sup>16</sup> Hz). The nuclei move also in an oscillatory manner and the nuclear coordinates ( $Q_j$ ) vary with frequency  $v_j$  such that  $Q_j = Q_j^0 \cos \left(2\pi \, v_j \, t\right)$ , where  $Q_j^0$  are the equilibrium coordinates of nucleus j and  $v_j$  the

frequency of the oscillation. The polarizability is dependent on the position of all the nuclei as we found above ( $\alpha = \alpha_o + \left(\frac{d\alpha}{dQ_j}\right)Q_j$ ). Hence, we can make a series of substitutions:

(The term substituted in each step is indicated in **bold** font)

$$\vec{\mu}_{ind} = \alpha \vec{E}_t = \alpha \vec{E}_0 \cos(2\pi v_0 t) = \alpha_o \vec{E}_0 \cos(2\pi v_0 t) + \left(\frac{d\alpha}{dQ_i}\right) Q_j \vec{E}_0 \cos(2\pi v_0 t)$$

$$\dot{\boldsymbol{\omega}} \alpha_o \vec{\boldsymbol{E}}_0 \cos \left( 2\pi \, \boldsymbol{v}_0 t \right) + \left( \frac{d \, \alpha}{d \, \boldsymbol{Q}_j} \right) \boldsymbol{Q}_j^0 \cos \left( 2\pi \, \boldsymbol{v}_j t \right) \vec{\boldsymbol{E}}_0 \cos \left( 2\pi \, \boldsymbol{v}_0 t \right)$$

$$\dot{c}\alpha_{o}\vec{E}_{0}\cos(2\pi v_{0}t) + Q_{j}^{0}\vec{E}_{0}\left(\frac{d\alpha}{dQ_{j}}\right)\cos(2\pi v_{j}t)\cos(2\pi v_{0}t)$$

remembering the identity:  $\cos A \cos B = \frac{\cos (A+B) + \cos (A-B)}{2}$ 

$$\vec{\mu}_{ind} = \alpha_o \vec{E}_0 \cos(2\pi v_0 t) + Q_j^0 \vec{E}_0 \left(\frac{d\alpha}{dQ_j}\right) \cos \vec{c} \vec{c}$$

Rayleigh anti-Stokes

Stokes

The first term corresponds to elastic or Rayleigh scattering, while the second and third term correspond to the anti-Stokes and Stokes scattering, respectively. This formulation is wholly classical and misses many of the details of Raman scattering but already we can see that the rate of change of

polarizability at the equilibrium nuclear coordinates 
$$\left\{\left(\frac{d\alpha}{dx}\right)_{x=0}\right\}$$
 must not be equal to zero.

Furthermore, the induced dipole moment (polarization) is linearly dependent on the strength of the electric field (laser).

#### 5.3. The Kramer-Heisenberg-Dirac (KHD) equation

The quantum mechanical treatment of polarizability  $(\alpha)$  can be carried out using the Kramer-Heisenberg-Dirac (KHD) equation, and differs from the classical description in the previous section in that it rationalizes the factors that influence its magnitude, in particular the dependence of polarizability on the wavelength of excitation and resonance enhancement. The wavelength dependence of the polarizability is derived from the KHD equation:

$$(\alpha_{\rho\sigma})_{GF} = k \left( \sum_{I} \frac{\langle \Psi_{R_{F}} | \hat{\mu}_{\rho} | \Psi_{R_{I}} \rangle \langle \Psi_{R_{I}} | \hat{\mu}_{\sigma} | \Psi_{R_{G}} \rangle}{\omega_{IG} - \omega_{hv} + i \Gamma_{IG}} + \sum_{I} \frac{\langle \Psi_{R_{I}} | \hat{\mu}_{\sigma} | \Psi_{R_{G}} \rangle \langle \Psi_{R_{F}} | \hat{\mu}_{\sigma} | \Psi_{R_{I}} \rangle}{\omega_{IF} + \omega_{hv} + i \Gamma_{If}} \right)$$

which describes the polarizability of a molecule, where  $\rho$  and  $\sigma$  are the polarization of the incident and scatter light and summed over all vibronic (vibrational-electronic) states of the molecule, with the subscripts G indicating the initial state, I the intermediate state, F the final state,  $\Psi_{R_c}$ ,  $\Psi_{R_I} \wedge \Psi_{R_F}$  are the ground, intermediate and final vibronic states, and  $\hat{\mu}_{\rho}$ ,  $\hat{\mu}_{\sigma}$  are the dipole moment operators going from the ground to intermediate and intermediate to final states, respectively (Rousseau, 1979). The first term is essentially mixing the ground, final and excited states, starting with the

ground state. The second term is almost the same but in the opposite direction. The sign in the denominators is important. In the first term, as the wavelength of excitation approaches the gap between ground and excited electronic states,  $\omega_{GI}$  and  $\omega_{ho}$  cancel each other and the term becomes very large. In contrast for the second term the denominator increases as the excitation wavelength shortens and the term decreases in importance.  $\Gamma$  is a damping factor which is introduced in both the KHD equation and the Heller formulism (see section 8.5.6.). The damping factor  $i\Gamma$  is related to the 'lifetime' of the electronically excited state. It represents the dephasing of the excited state wavepacket that occurs due to other degrees of freedom and  $1/\Gamma$  is typically a few vibrational periods. Importantly it prevents the denominator from becoming 0 (which would result in infinite polarizability!).

The wavefunctions can be simplified by applying the Born Oppenheimer approximation (that nuclei do not move on the timescale that electrons move) and the nuclear and rotational components can be separated (and the rotational part neglected for simplicity). The electronic component is described with the term  $M_{IG}(R_{x=0})$  with  $M_{IG}(R_{x=0})$  as a correction factor and  $R_{\varepsilon}$  describes the movement from the equilibrium position. The three terms are referred to as the A, B and C (not shown) terms:

$$(\alpha_{\rho\sigma})_{GF} = k \, M_{IG}^2 (R_{x=0}) \sum_{I} \frac{\langle \Phi_{R_F} \big| \Phi_{R_I} \rangle \langle \Phi_{R_I} \big| \Phi_{R_G} \rangle}{\omega_{IG} - \omega_{hv} + i \, \Gamma_{IG}} + k \, M_{IG} (R_{x=0}) \, M_{IG}^{'} (R_{x=0}) \sum_{I} \frac{\langle \Phi_{R_F} \big| \Phi_{R_I} \rangle \langle \Phi_{R_I} \big| R_{\varepsilon} \big| \Phi_{R_G} \rangle + \langle \Phi_{R_F} \big| R_{\varepsilon} \big| \Phi_{R_I} \rangle \langle \Phi_{R_I} \big| \Phi_{R_$$

The first (A) term has as numerator the Frank-Condon factors, the overlap between the vibrational wavefunctions in the ground and excited states,  $\langle \Phi_{R_e} | \Phi_{R_i} \rangle \langle \Phi_{R_i} | \Phi_{R_c} \rangle$ .

If the potential wells of the ground and excited states are identical i.e. there is no difference in bond length (mean nuclear coordinates,  $\Delta Q > 0$ ) or force constant (bonds involved in the mode get either stronger or weaker,  $\Delta k > 0$ ) between the ground and excited electronic states, then this term is equal to zero (no-overlap) unless the ground and final states are the same. Hence, the A term contributes to polarizability primarily in the case of Rayleigh scattering.

The importance of this term to Raman scattering increases, however, as the wavelength of excitation approaches resonance with the electronic transition. The importance is apparent from consideration of the denominator  $\omega_{GI}-\omega_{hv}$ , which makes the whole term increase rapidly as  $\omega_{hv}$  approaches  $\omega_{GI}$ . If the equilibrium bond lengths and or force constant is different between the ground and electronically excited state that comes into resonance with the excitation laser, then the overlap between the ground and final states that are not the same becomes non-zero also. This provides for intensity of Raman scattering only for those modes that are distorted in the excited state.

Finally, the first term contains  $M_{IG}^2(R_{x=0})$  (which is  $\langle \psi_e | \mu | \psi_g \rangle^2$ ), and hence the magnitude of the Aterm is dependent on the square of the electric dipole transition moment (manifested in the molar absorptivity). Taken together the two terms indicate that the increase in polarizability and hence resonant enhancement is dependent on the 'allowedness' of the electronic transition.

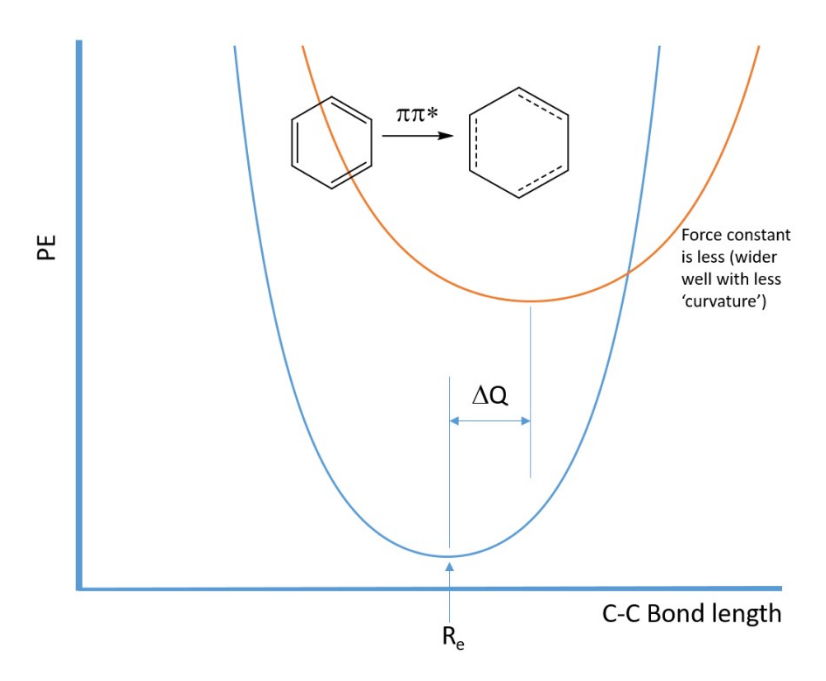


Figure 18. A change in equilibrium bond length and/or force constant between the ground and excited state is required for the band associated with that normal mode to undergo resonance enhancement.

The second (B) term includes contributions to the polarizability due to vibronic coupling between excited electronic states (i.e.  $\psi_e \wedge \psi_s$ ). This term is important only when the two electronic states are close in energy ( $\Delta E$  in the dominator) and the transition dipole moments between the ground state and each of the excited states is non-zero (i.e. both transitions are allowed). The components in the numerator are also important to consider, since  $\langle v|Q_j|m\rangle$  and  $\langle v|Q_j|n\rangle$  connect the ground ( $\psi_g$ ) and excited ( $\psi_e$ ) states that differ by one vibrational quantum. Importantly when they are multiplied by the Franck Condon factors (e.g.,  $\langle \Phi_{R_p}|\Phi_{R_l}\rangle$ ) for vibrational states that have the same quantum numbers then they do not vanish (go to zero) even if the excited state displacement is equal to zero ( $\Delta Q = 0$ ). Hence both totally and non-totally symmetric modes can be enhanced. The C term is omitted above and for a detailed description the interested reader is referred to the original paper by Albrecht (Albrecht 1961).

In summary, under non-resonant conditions the A-term provides for Rayleigh scattering and not Raman scattering (since it is zero if the initial and final vibronic states are not the same) and it is the B-term that contributes most to polarizability and hence Raman scattering. When the laser used is resonant with an electronic absorption band both A and B terms contribute to the intensity with the A-term dominating.

### 5.4. A-, B-, C-term enhancement mechanisms, overtones and combination bands

The mathematical basis for the theory of resonance enhancement of Raman scattering (Czernuszewicz and Spiro 1999) is beyond the scope of this chapter. However, the conclusions reached by Albrecht (Albrecht 1961), using the Herzberg-Teller formalism to treat the quantum mechanical description of dispersion, are important in regard to the excitation wavelength dependence of resonance Raman spectroscopy and its use in probing the electronic structure of chromophores.

The enhancement of Raman scattering from a compound near or at resonance conditions is typically due to the so-called A-term enhancement. The primary consideration is the difference in mean nuclear coordinates (Q, i.e. bond lengths/dihedral angles) between the ground electronic state and the electronically excited state that is in resonance with the excitation laser ( $\Delta E = hv_{exc}$ ). The enhancement is also proportional to the electric dipole transition moment for the electronic transition, and hence, the more allowed the electronic transition, the greater the expected enhancement. This is in part why porphyrins give intense resonantly enhanced Raman spectra when excitation is into their allowed  $\pi$ - $\pi$ \* transitions but the d-d bands of metal complexes do not provide significant enhancement.

#### 5.5. Assigning electronic absorption spectra

The assignment of localization of electronic transitions in UV/Vis absorption spectra is an important application of resonance Raman spectroscopy. An example of this can be seen in the hetereoleptic Ru(II) polypyridyl complex shown in Figure 19. The visible absorption spectrum shows two main transitions at ca. 420 and 550 nm. These visible absorption bands are metal to ligand charge transfer in nature ( $^{1}$ MLCT), however the excitations are relatively localized. Specifically the electron is excited from the  $t_{2g}$  orbitals of the Ru(II) ion to a ligand  $\pi^*$  orbital ( $\pi^* \leftarrow t_{2g}$ ). The complex [Ru(bipy)<sub>2</sub>(Me-Phpztr)]<sup>2+</sup> in this case contains two equivalent 2,2'-bipyridine ligands (bipy, shown in black) and a third ligand comprised of a methylated cationic pyrazine (shown in red) and an anionic 1,2,4-triazole moiety (shown in blue). Raman spectra recorded between 355 and 561 nm are shown in Figure 19.

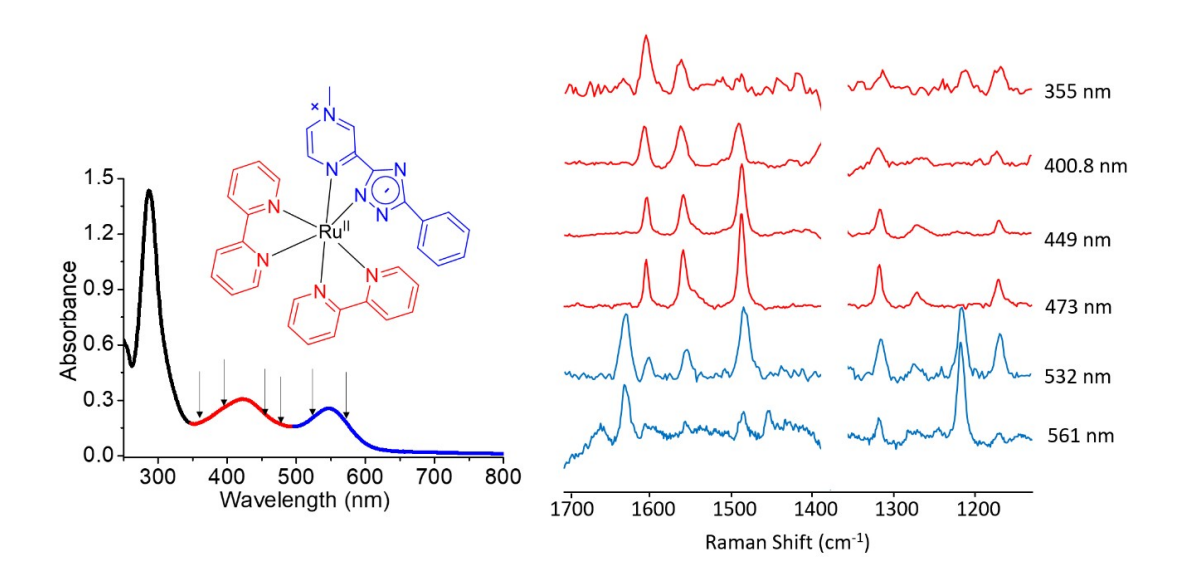


Figure 19. UV/Vis absorption spectrum of a hetereoleptic (not all ligands are the same) ruthenium(II) polypyridyl complex (shown as inset) and Raman spectra recorded at the indicated wavelengths (Draksharapu, et al. 2012).

The spectra obtained at 355, 400.8, 449 and 473 nm are essentially identical to those expected for the homoleptic (*all ligands are the same*) complex  $[Ru(bipy)_3]^{2+}$  (Figure 12). In all four spectra, the relative intensities of the bands change but their positions do not. The assignment of these bands as due to enhancement of Raman scattering from the bipy ligands was confirmed from the shifts induced by deuteration of the ligands (i.e. with d<sub>8</sub>-bipy all bands underwent a shift to lower wavenumbers). At 532 nm intense bands at ca. 1630 and 1240 cm<sup>-1</sup> are observed also and at 561 nm these are the only bands that are enhanced significantly. These additional bands are assigned to the methylated pyrazine moiety based on shifts induced by isotope labeling also. These data allowed us

to assign the low energy absorption as being predominantly  ${}^{1}MLCT$  (pz $\leftarrow$ t<sub>2g</sub>) and the absorption at 420 nm as  ${}^{1}MLCT$  (bipy $\leftarrow$ t<sub>2g</sub>).

The wavelength dependence of the resonance Raman spectrum in this case highlights an essential point in resonance enhancement. In essence the basis of the simplifications made by Heller in establishing a theoretical basis for Raman and resonance Raman spectroscopy (see below). The charge transfer transition involves formal one electron reduction of a ligand or ligand moiety. The reduction involves population of an anti-bonding orbital and hence there are substantial changes to bond order and equilibrium bond lengths, i.e.  $\Delta Q > 0$ . A non-zero value of  $\Delta Q$  is an essential requirement for A-term enhancement. For the other ligands, the change in oxidation state of the metal center has relatively little effect since the electron is taken formally from a non-bonding orbital. Hence in the electronically excited state, the other ligands are unchanged in terms of bond lengths and strengths and hence  $\Delta Q = 0$ . As a result there is no mechanism for their Raman scattering to be enhanced.

A second mechanism for enhancement of Raman scattering is through vibronic coupling between two electronically excited states. Only modes that are responsible for the coupling are enhanced, which are often non-totally symmetric modes. Bands that are only weakly enhanced at some wavelengths can become intense at other wavelengths depending on the electronic excited state structure. The enhancement of non-totally symmetric modes (e.g.,  $A_{2g}$ ,  $B_{1g}$ ,  $B_{2g}$  in porphyrins) is consistent with vibronic bands in the absorption spectrum. Non-totally symmetric modes are identifiable by the 'anomalous polarization'; i.e. if the laser used is plane polarized then Raman scattering under resonance conditions should be polarized also, however B-term enhancement is characterized by some Raman bands not being polarized.

The third mechanism for enhancement is referred to as C-Term enhancement (this term is not usually included in the form of the KHD equation above), and is much less commonly encountered. It becomes important when the excitation wavelength used is resonant with a vibronic side band of a forbidden or weakly allowed electronic absorption band such as the Q-bands of porphyrins, which although forbidden 'borrow' intensity from the allowed Soret transition.

Without going into detail, the C-term is proportional to two integrals that depend on Q (nuclear coordinates) and connect vibrational levels in the ground  $\dot{c}g$  and electronically  $\dot{c}e$  excited states that differ by one quantum of angular momentum – hence overtones are enhanced.

$$C \propto \langle m|Q|v\rangle \cdot \langle v|Q|n\rangle$$

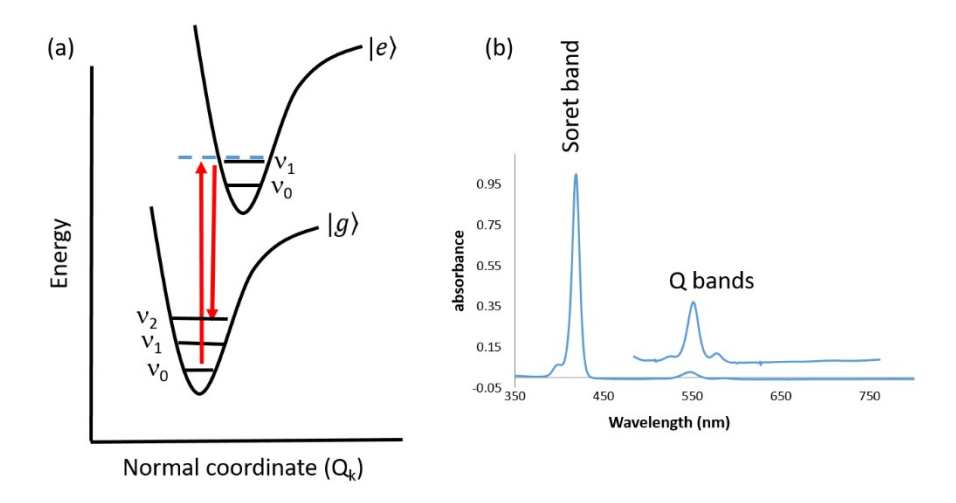


Figure 20. (a) C-term enhancement allows for significant intensity for overtones, when excitation is in resonance with the second vibrational level of an excited state. (b) UV/vis absorption spectrum of Zinc tetraphenylporphyrin in dichloromethane.

Raman spectroscopy of porphyrins and related compounds is a well-established field in itself due primarily to the strong resonant enhancement observed upon excitation across their visible absorption spectra. At certain wavelengths the spectra become much more complex than expected due to enhancement of overtones (Paulat, et al. 2006).

A characteristic of C-Term enhancement is the enhancement of overtones and combination bands which is seen in spectra of porphyrins when excited into the  $Q_v$  region of their absorption spectra. Such enhancement is notable because, in contrast to FTIR spectroscopy, overtones and combination bands are generally absent or weak in Raman spectra, and especially resonantly enhanced Raman spectra. The observation of overtones and combination bands is most likely for modes that undergo the largest displacements in the electronically excited states and when  $\Gamma$  is large. An example of this effect is in Raman spectra of an Fe(IV)=O complex reported by Que and coworkers where the 1<sup>st</sup> overtone of the 798 cm<sup>-1</sup> stretching mode appears at 1587 cm<sup>-1</sup>, and, importantly, shows the expected sensitivity to <sup>18</sup>O labelling (see Van Heuvelen et al. 2012).

#### 5.6. Heller's time dependent approach

Polarizability can, in principle, be calculated using the KHD equation, in which all vibronic (vibrational-electronic) states are included. In practice these calculations are prohibitively large and expensive in computational time even for small molecules. However, the time independent approach taken in the KHD equation is a useful start point for the time dependent approach in which the calculation of polarizability is simplified considerably by taking a semi-classical approach as proposed by Eric Heller (Heller, 1981).

In the Heller approach, the problem of the breakdown in the Born-Oppenheimer approximation is reduced by considering how the nuclei move during the excitation. As discussed above, the Frank-Condon principle states that electrons and nuclei move at different speeds and therefore all electronic transitions are vertical with respect to nuclear coordinates – i.e. the nuclei do not move to an appreciable extent on the time scale over which the electronic distribution in the molecule is changed by an oscillating electric field.

After excitation, the nuclei feel a new force field and as a result begin to move to reach a new set of nuclear coordinates that minimizes the energy of the system. The distribution of the nuclei once the electronically excited state is reached is essentially that of the ground state, in other words the molecules are in an excited 'virtual' state (Figure 21) called a 'wavepacket'. Electronic transitions can be described by the overlap of the time independent vibrational wavefunctions (eigenfunctions) to form a wavepacket. The wavepacket begins to 'move' along the excited state surface – or rather the nuclei in each molecule begin move towards their new equilibrium positions with a speed corresponding to the frequency of the normal modes that bring them to these new nuclear coordinates. Put another way, only those modes associated with bonds that differ in length between the ground and excited state are involved in this process.

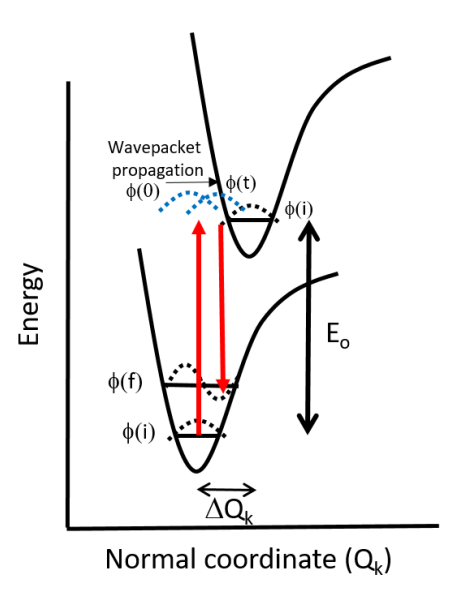


Figure 21. Excitation from the ground state leads to a virtual state which has the same vibrational wavefunction (called a wavepacket) as the ground state. The wavepacket changes due to nuclear motion, and would ultimately evolve to a stationary state of the excited state except if it were not relax back to the ground state instanteously with generation of a scattered photon.

If we consider the ground and excited states involved in an electronic transition the initially formed vibrational wavefunction in the exicted state is the displaced wavepacket  $\phi(0)$ , which is equal to the ground state vibrational wavefunction multiplied by the transition dipole operator. For simplicity, we will disregard direction and orientation aspects; i.e. the polarization of the incoming photons with respect to molecular axes.

The frequency dependence of the polarizability, with a single excited state involved, is given by the KHD equation, which can be expressed, when only one excited state is considered (Heller et al. 1982, by two terms (resonant and non-resonant):

$$\alpha_{0\rightarrow n}(\omega) = \sum_{k} \frac{\langle \psi_{n} | \mu | \psi_{k} \rangle \langle \psi_{k} | \mu | \psi_{o} \rangle}{(E_{k} - E_{0}) - \hbar \omega + i \Gamma} + \sum_{k} \frac{\langle \psi_{n} | \mu | \psi_{k} \rangle \langle \psi_{k} | \mu | \psi_{o} \rangle}{(E_{k} - E_{0}) + \hbar \omega + i \Gamma}$$

(resonant term)+(nonresonant term)

Where  $\psi_o$  is the ground vibrational state,  $\psi_n$  is the n<sup>th</sup> vibrational state,  $\omega$  is the frequency of the incoming photons,  $\psi_k$  is the k<sup>th</sup> vibrational eigenstate (wavefunction) in the excited state and E<sub>k</sub> is the

energy of that state. Note that this equation is essentially a repeat of the KHD equation mentioned at the beginning of section 8.5.3.

For large molecules only a small part of the excited state potential surface is of relevance, since only a few of the nuclei in the molecule are displaced in the exicted state. Hence an alternative equation, proposed by Heller and coworkers, can be applied that limits the number of states involved and considers the evaluation of the wavepacket with time:

The polarisability with respect to a specific frequency is given by:

$$\alpha_{0\rightarrow n}(\omega) = \int_{0}^{\infty} e^{i\omega t - \Gamma t} \langle \phi_{n} | \phi(t) \rangle dt + (nonresonant term)$$

Where  $\[ \dot{c} \ \phi \] = \mu \lor \psi \[ 0 \] \]$  and  $\[ \dot{c} \ \phi_n \] = \mu \lor \psi \[ n \] \]$  and  $\[ \phi \[ t \] \]$  is the same wavepacket at any point over time. The Raman scattering into a given final state n is proportional to the square of the amplitude. Even though the integration is from 0 to infinity the actual integration is only necessary over short time periods due to dephasing and less obviously if the excitation frequency is moved away from resonance then the uncertainty principle  $\Delta\omega\tau$  is approximately equal to 1 where  $\Delta\omega$  is the deviation from resonance and  $\tau$  is lifetime of the wavepacket in the excited state; i.e. before the relaxation to the ground electronic surface takes place.

#### 6. SERS and SERRS spectroscopy

In SERS (Surface Enhanced Raman Scattering) and SERRS (Surface Enhanced resonance Raman Scattering) spectrum employ nanostructured noble metals (principally silver and gold) are used to enhance Raman scattering by several orders of magnitude. SERS spectroscopy is used extensively in analytical applications and especially in sensor applications. The technique is relatively simple to implement and surface enhanced spectra of compounds are obtained upon aggregation of aqueous gold or silver colloids by addition of anions (Cl<sup>-</sup>, SO<sub>4</sub><sup>2-</sup> etc.) or using nanostructured surfaces. Analyte that is present between the contacting (aggregating) nanoparticles benefit from a so called antennae effect, arising from the intense electric field formed between the particles.

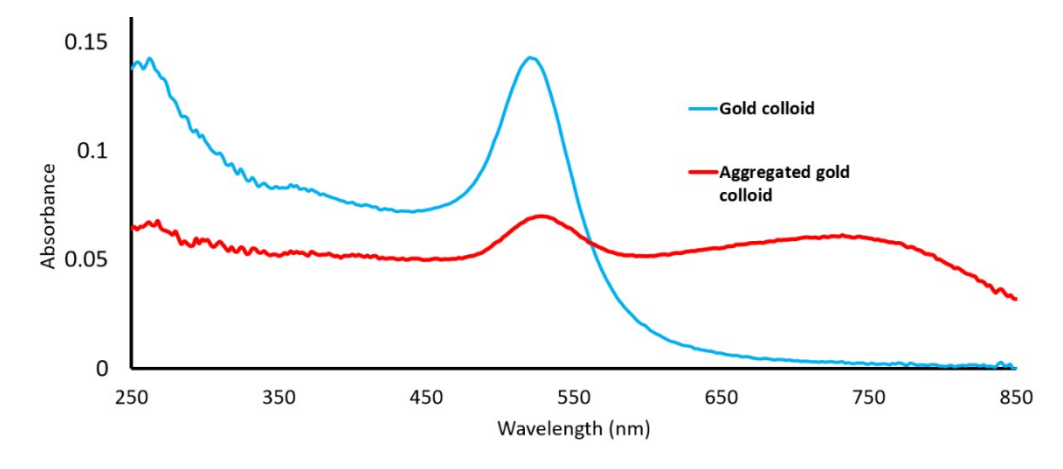


Figure 22. UV/vis absorption spectrum of a gold colloid before and shortly after addition of KCl(aq) to induce aggregation.

As for resonantly enhancement due to the coincidence of the laser wavelength with an electronic absorption band of the analyte, in SERS spectroscopy the aggregation is optimized to shift the surface plasmon resonance of the colloid to be coincident with the laser used (typically 632.8 nm or 785 nm). If the analyte itself has an electronic absorption band at the wavelength of excitation, then

enhancement of Raman scattering due both to the surface and resonance enhancement as discussed above is expected.

A key challenge to the application of SERS in (bio)inorganic chemistry is the non-innocence of the gold and silver colloids, and especially the gold and silver ions present unavoidably in solution. As an example, the SERS spectra of two copper(II) complexes obtained using gold colloid are shown in figure 23. It is clear from comparison with the SERS spectra obtained with the ligands only that the spectra are in fact of the gold(I) complexes and not of the original copper(II) complexes. Indeed, any analyte that is a metal complex in which the ligand is labile, or which bear functional groups that can bind to gold or silver (e.g. N, S, alkynes etc), will likely provide a spectrum of a gold or silver complex rather than the original form of the analyte.

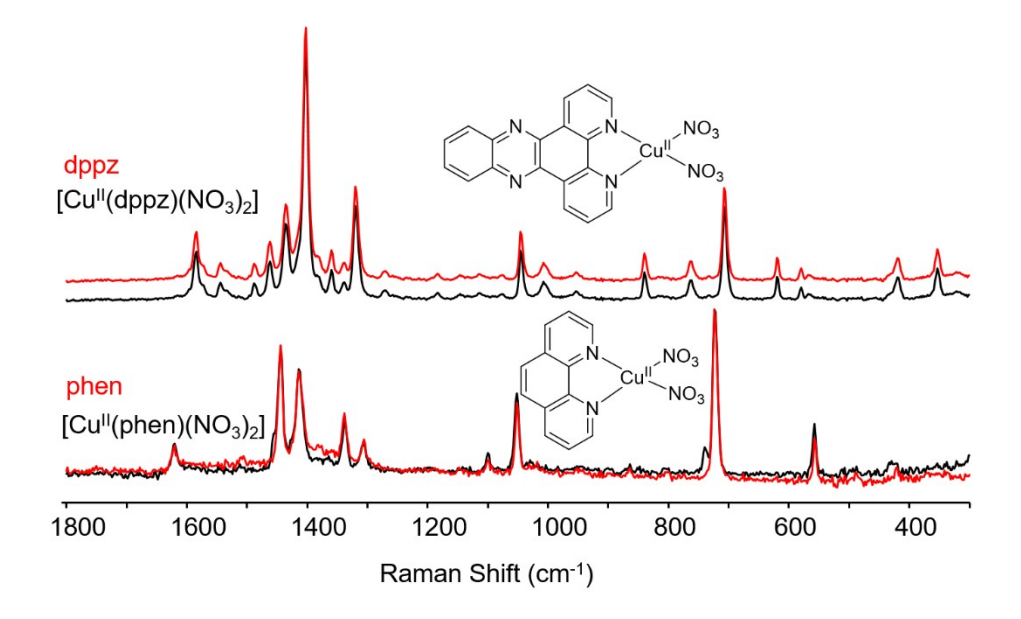


Figure 23. SERS spectra of both copper(II) complexes (black) and of the ligands alone (red) on aggregated gold colloid. The spectra are identical and are distinct from the solid state spectra of either the complexes or ligands in terms of band positions, confirming that the spectra are of the gold complexes of the ligands.

The interaction of analytes with the colloid can have a positive effect with regard to fluorescence, which can swamp the weak Raman signal. Often the colloid quenches the excited states of bound molecules and reduces interference from fluorescence, while providing enhancement of the Raman spectrum.

#### 7. Experimental and instrumental considerations

#### 7.1. Isotope labelling and band assignment

The assignment of Raman spectra is relatively straightforward, given that the band positions for particular types of normal modes (vibrations) are the same as found in FTIR spectra. Indeed the tables available for IR spectroscopy can be used equally well for Raman spectroscopy. The only real caveat to this is that the relative intensities of Raman bands do not correspond with those in IR spectra. More recently DFT methods have developed to a sufficiently sophisticated level that we can accurately predict vibrational spectra.

In the studies in which resonant enhancement is of interest, we generally know the structure of the compound under study already. Often we want to confirm that a particular band is assigned

correctly and in this, isotope labelling is especially useful, given that a primary use of Raman spectroscopy in bioinorganic chemistry is in determining the frequency and hence force constant for key bond classes (e.g. O-O, Fe-O.. stretching, etc.). Indeed, isotope labelling is a key tool in the definitive assignment of bands in species that are otherwise not sufficiently stable to be isolated.

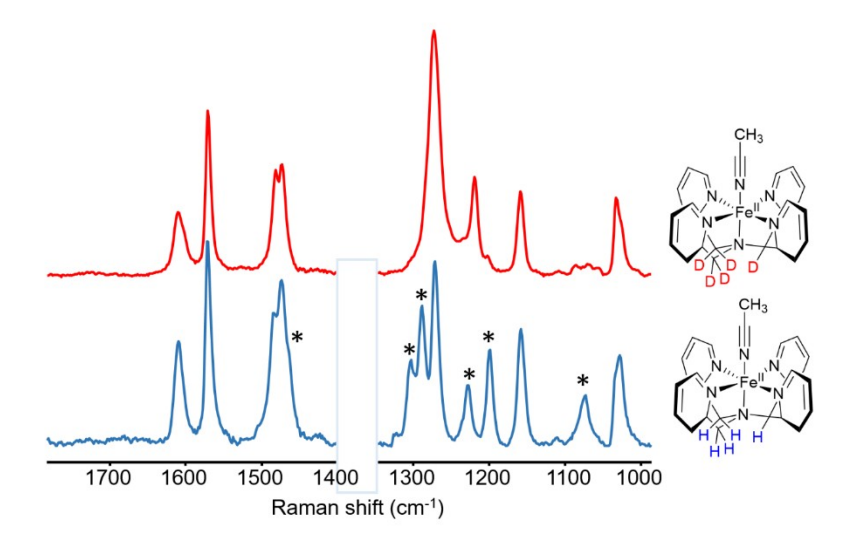


Figure 24. The effect of deuteration of the benzylic positions of an iron binding ligand on the resonance Raman spectrum of its low spin Fe(II) complex. Note that the bands at 1600 cm<sup>-1</sup> are essentially unaffected but the aliphatic in and out of plane modes at ca. 1250 cm<sup>-1</sup> are changed dramatically by the deuteration (Draksharapu, et al. 2012).\*bands shifted by deuteration.

An example of the use of resonance enhanced Raman spectroscopy in bioinorganic and biomimetic chemistry, and the role played by isotope labelling, is in the study of species formed upon the reaction of iron complexes with oxidants such as oxygen and hydrogen peroxide. The species of interest are typically Fe(III)-OOH, Fe(III)O<sub>2</sub> and Fe(IV)=O intermediates, for example an Fe(III)-OOH species is the last detectable intermediate in the oxidative cycle of the DNA cleaving anti-cancer drug Bleomycin. Until relatively recently, these species had not been isolated and characterised structurally and their near-infrared absorption bands around 600 to 850 nm has allowed us to use resonance enhancement to determine the strength of the Fe(IV)=O and O-O bonds, which can be related to the reactivity of the complexes.

In the example below, an Fe(III)-OCl complex is formed by reaction of an Fe(II) complex with sodium hypochlorite. Four bands are enhanced resonantly at the wavelength of excitation used, with the band at ca. 845 cm<sup>-1</sup> undergoing the expected shift for an Fe(IV)=O species formed under these conditions also (Figure 25). The other three bands are due to the Fe(III)-OCl species formed and exchange of <sup>16</sup>O with <sup>18</sup>O shows that only two bands undergo a shift in wavenumber. The band at ca. 670 cm<sup>-1</sup> is not sensitive to oxygen labelling as it is due a Fe-N stretching mode. The other two bands undergo a shift consistent with their assignment as Fe-O and O-Cl stretching modes. DFT methods allow for the prediction of both their wavenumber shift and the isotope shift. This example illustrates that vibrational modes are essentially localised over a few atoms (two or three typically) and in this case the excitation is into a ligand to metal charge transfer band of the complex, in which the iron formally changes from Fe(III) to an Fe(III) oxidation state. The iron-ligand bond lengths differ in the two oxidation states and as a result there is a change in nuclear coordinate ( $\Delta Q_j \neq 0$ ). The resonance enhancement, however, is modest (approximately 10 to 50 times) which reflects the forbidden nature of the transition.

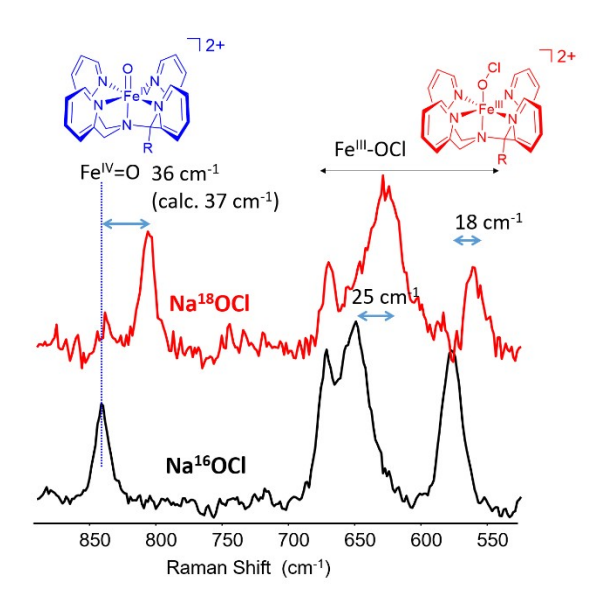


Figure 25. Raman spectrum of an Fe(III)-OCl species generated in solution by addition of NaOCl to the Fe(II) complex. Replacement of  $H_2^{16}O$  with  $H_2^{18}O$  results in shifts of some but not all bands (Draksharapu, Angelone et al. 2015).

#### 7.2. Resolution and natural line width

In many cases, Raman spectroscopy is employed to monitor changes in conditions (e.g., binding or release of a ligand, change in oxidation state etc.). The change in the spectrum must be beyond its resolution limit to begin with but often when changes are minor it falls to the experience of the spectroscopist to discern whether the changes are due to the species under study or simply due to instrumental/optical properties. Furthermore, although modern instrumentation can achieve resolutions as low as 0.1 cm<sup>-1</sup>, this is only useful for samples in the gas phase and the real limit to resolution in studies in condensed phases (liquids and solids) is determined by natural line widths (6-8 cm<sup>-1</sup>).

#### 7.3. Confocality, the inner filter effect, and quartz

A key aspect of Raman spectroscopy is that it is inherently a confocal technique, i.e. the Raman spectrum measured is due to scattering from a small volume of space called the confocal volume (Figure 26).

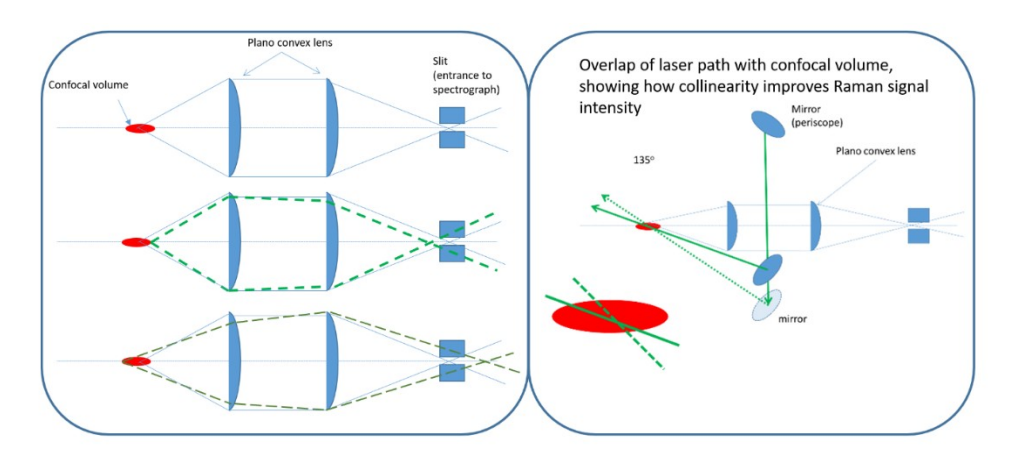


Figure 26. The light scattered during the passage of a laser through a sample is largely lost except for a small volume (the confocal volume in red). Light emanating from this region is collected by a lens and refocused into the spectrograph (through the slits).

Resonance Raman spectroscopy presents an experimental dichotomy that can limit application in some cases. An optical absorption at the wavelength of excitation is required in order to achieve resonance enhancement. However, if the confocal volume of the Raman system is at the center of a 1 cm pathlength cuvette then the laser undergoes attenuation (absorption) before it reaches the confocal volume. Furthermore the Raman scattering has to pass through 5 mm of the sample along the path to the collection optics. Hence, although an increase in analyte concentration increases the (resonance) Raman intensity relative to the solvent bands, the concomitant increase in absorbance leads to an overall reduction in the intensity of the spectrum. In short, sometimes less is more in Raman spectroscopy. An example of this effect is shown for a manganese complex in Figure 27.

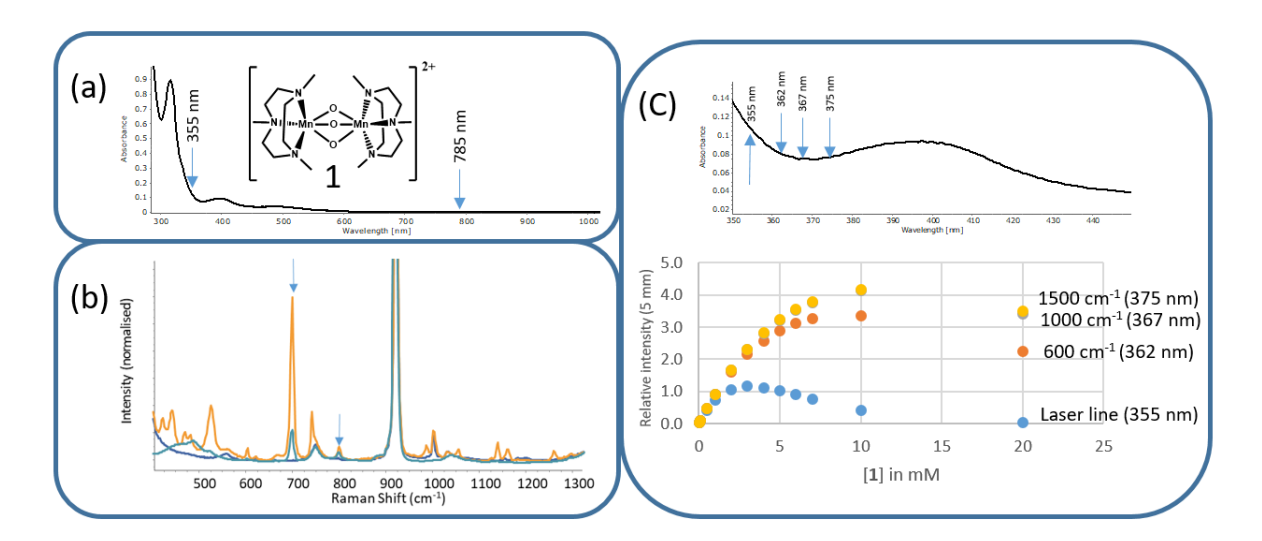


Figure 27. UV/vis absorption spectrum of manganese complex **1** (1 mM in CH<sub>3</sub>CN, 1 mm pathlength) showing positions of selected Raman bands with excitation at 355 nm. (b) Raman spectrum at  $\lambda_{\rm exc}$  785 nm of CH<sub>3</sub>CN (blue), of **1** (0.1 M in CH<sub>3</sub>CN, yellow) and at  $\lambda_{\rm exc}$  355 nm of **1** (0.001 M in CH<sub>3</sub>CN, green). The two resonantly enhanced bands of **1** are indicated with arrows – the enhancement factor is estimated as 16 for the band at 700 cm<sup>-1</sup> and 50 for the band at 800 cm<sup>-1</sup>. (c) Calculated relative intensity of the laser at the center of a 1 cm pathlength cuvette and Raman bands at selected Raman shifts for excitation at 355 nm as a function of concentration. The overall loss in signal intensity in this example is due to the inability of the laser to penetrate the solution, and maximum absolute Raman signal is expected at ca. 4-6 mM.

A major consideration in resonance Raman spectroscopy is the inner filter effect; the reabsorption of scattered light before it leaves the cuvette (see also figure 11b). As the absorbance of a sample increases there is a tendency to focus at or near the edge of the sample holder (quartz cuvette or glass capillary etc) and since the penetration of light can be quite limited (for example for an absorbance of 2, the laser is only 10% its initial power by the time it reaches the center of the 1 cm cuvette). Increasing the absorbance to 3 in a 1 cm pathlength cuvette means that within 1 mm, 50% of the light has been absorbed. In such situations positioning the cuvette so that the confocal volume contains only the first millimeters of solution can reduce the impact of the inner filter effect. However, this also means that the quartz or glass walls of the cuvette are within the confocal volume and Raman scattering from these materials will appear in the spectrum also. A key difficulty is that

these bands are broad and are difficult to remove by subtraction, and are especially a problem in studies where isotope shifts in the <1000 cm<sup>-1</sup> region are concerned (figure 28).

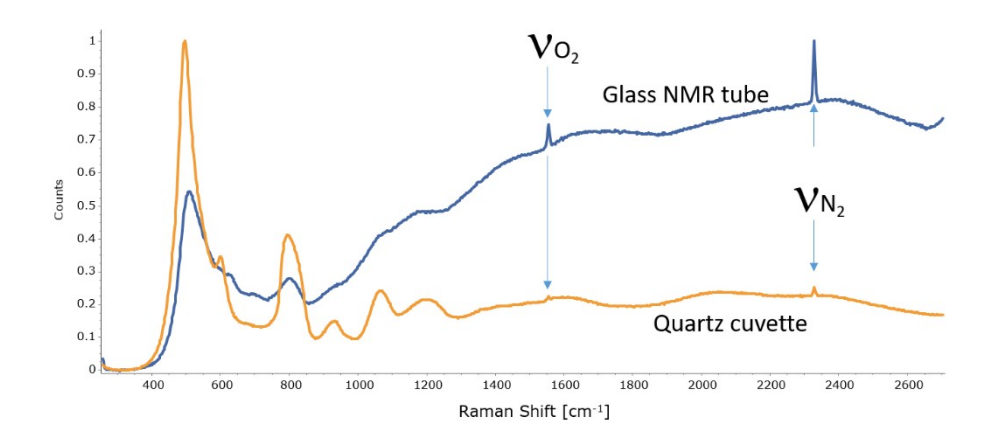


Figure 28. Raman spectrum of an empty NMR tube and an empty quartz cuvette in which the wall of the cuvette is positioned with the confocal volume.

As a final point of warning that is especially relevant when operating under resonance conditions, it should not be overlooked that the intense highly focused lasers used in Raman spectroscopy can be quite good at inducing photochemical reactions. In many cases it is not possible to obtain resonance Raman spectra simply because the sample has been obliterated before a spectrum can be acquired. In these cases cooling, continuous flow systems, and sensitive detectors that allow for low laser powers to be used, are essential tools.

#### 8. Applications of resonance Raman spectroscopy

In this last section a number of examples of the application of resonance enhancement of Raman scattering (so called resonance Raman spectroscopy) are discussed. The goal is not to be comprehensive but instead give an impression of both the ease with which the technique can be applied and its potential to help solve problems.

## 8.1. Resonantly enhanced Raman spectroscopy in the characterization of artificial metalloenzymes based on the LmrR protein

Resonance Raman spectroscopy, as it is often termed, is a useful asset in studies under biologically relevant conditions, i.e. in aqueous buffers, when the compound or moiety of interest is present only at low concentrations. Provided that the compound absorbs light at a convenient wavelength (and by convenient we mean a wavelength close to the wavelengths of the lasers available in one's own or a friend's laboratory!), and that absorbance is appreciable (greater than 0.2), then it may be possible to study the compound or moiety under conditions relevant to its application.

The LmrR protein, a protein that lends multidrug resistance to bacteria, has been applied by the Roelfes group over the last years as a basis for artificial metalloenzymes (Drienovska, et al. 2015). An artificial metalloenzyme is one in which a protein is modified with, for example, a non-natural amino acid that allows it to bind a metal ion. In the case of the LmrR protein, the Roelfes group replaced an amino acid (phenylalanine) with an amino acid that bore a 2,2'-bipyridyl unit instead of the phenyl of phenylalanine. The 2,2'-bipyridyl unit is positioned by the amino acid sequence within the pocket formed by the symmetric dimeric LmrR protein, and should in principle be able to bind two Cu(II) ions. The copper(II) ions then act as Lewis acid catalysts with the chiral hydrophobic pocket of the protein to engage in enantioselective catalytic reactions.

Proving that binding to the 2,2'-bipyridyl takes place selectively, however, is challenging since the Cu(II) ions can bind to other residues around the protein both inside and outside of the pocket. Direct spectroscopic evidence under reaction conditions is ideal, however, the absorption spectrum of the copper(II) bound LmrR protein shows overlap of the absorption bands of the protein (which contains tryptophan residues) and the expected absorption of the Cu(II) 2,2'-bipyridyl complex. Furthermore, the concentration of the protein available was ca. 60  $\mu$ M.

The optimum wavelength for achieving resonance enhancement of Raman scattering of the Cu(II) 2,2'-bipyridyl complexes is 355 nm, however, the use of pulsed laser sources (i.e. Nd-YAG laser) with proteins leads to laser induced aggregation and precipitation. Continuous wave (CW) lasers are available, and in this case the limits of detection for the Cu(II) 2,2-bipyridyl complex were determined to be ca. 20 mM using NO<sub>3</sub><sup>-</sup> (which does not show resonance enhancement) as well as the water Raman band as internal reference. The weak Raman scattering cross-section of water in this case is an enormous advantage, as the strong scattering from organic solvents would have overwhelmed the weak signals of the complex. Comparison with the Raman spectrum obtained for the LmrR Cu(II) complex was hampered by fluorescence due to residual contaminants remaining after protein purification (see 8.4.2.). Although the fluorescence signal is broad and can be removed by a simple background correction, the primary source of noise in Raman spectroscopy is shot noise as (*shot noise*  $\propto \sqrt{signal}$ ), which is detrimental to the limit of detection. Nevertheless, comparison of the spectrum of the *in situ* prepared Cu(II) 2,2'-bipyridyl complex in MOPs buffer with that of the spectra of the native and the 2,2'-bipyridyl modified LmrR protein in the presence and, absence of Cu(II) ions, shows that the Cu(II) ions bind predominantly to the 2,2'-bipyridyl residues.

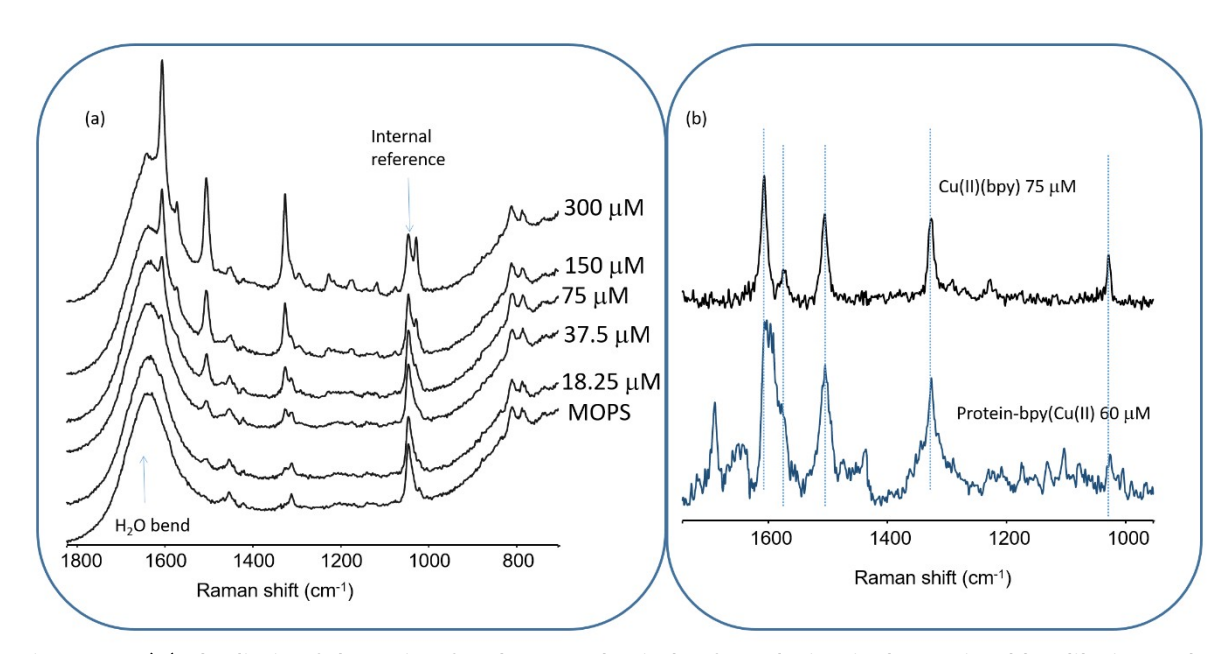


Figure 29. (a) The limit of detection for the complex in buffer solution is determined by dilution to be ca. 20  $\mu$ M. (b) Using the NO<sub>3</sub> anion as an internal reference allows for accurate estimation of the concentration of copper(II) complex formed in the protein by comparison.

In this example, the resonance enhancement of Raman scattering is applied to confirm the formation of a species under reaction conditions rather than to assign spectra or probe electronic structure. Importantly it has to be emphasized that the experiment was carried out as any Raman spectrum would be recorded, apart from selection of the laser wavelength to coincide with an optical absorption band of the chromophore of interest.

#### 8.2. Reaction monitoring with resonance Raman spectroscopy

The ability to obtain Raman spectra of compounds present at low concentration is a key advantage of the effect of resonance enhancement in the study of reaction mechanisms. As an example, we will take a manganese catalyzed oxidation of alkenes with  $H_2O_2$  (Figure 30). The concentration of the catalyst, [Mn(IV)<sub>2</sub>O<sub>3</sub>(tmtacn)<sub>2</sub>]<sup>2+</sup>, used in this example is 1 mM and, as it is in a high oxidation state, its UV/Vis absorption spectrum allows for the observation of the catalyst's conversion to the complex [Mn(III)<sub>2</sub>O(μ-O<sub>2</sub>CR)<sub>3</sub>(tmtacn)<sub>2</sub>]<sup>2+</sup> under reaction conditions. Despite the extensive visible absorption of both species, the Raman scattering of either complex is not enhanced when the laser wavelength is between 457 and 785 nm. However, this is consistent with the assignment of these bands as being largely metal centered (MC) transitions and therefore excitation does not affect the Mn-ligand or ligand bond lengths or strengths significantly. By contrast excitation at 355 nm results in enhancement of some of the Mn-O-Mn modes for both complexes, consistent with the ligand (oxo) to metal charge transfer character of the bands since the charge transfer in the excited state involves a change in Mn-O bond strength and hence length. In this example, the enhancement due to resonance is approximately 50 to 100 times only and illustrates that even a small increase in signal can be sufficient to obtain useful data. The ability to determine the concentration of both complexes with good accuracy, as well as that of H<sub>2</sub>O<sub>2</sub>, allows for direct comparison over time of the changes in the concentration of each.

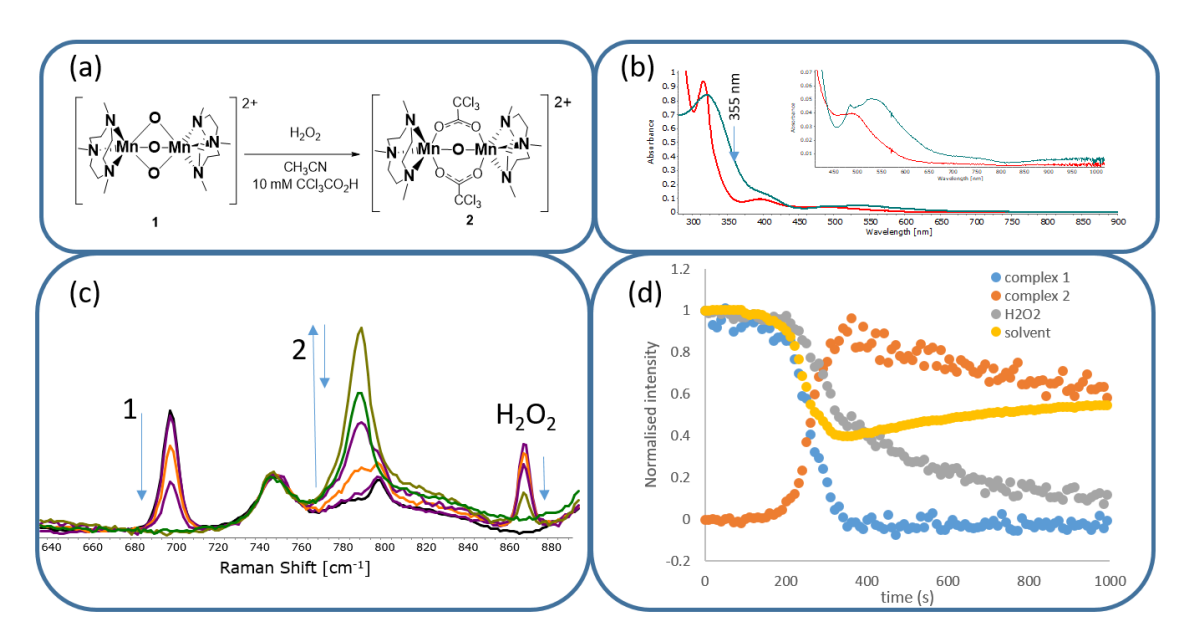


Figure 30. (a) Conversion of **1** to **2** with  $H_2O_2$  and (b) UV/vis absorption spectra of **1** (red) and after conversion to **2** (black, 1 mM in  $CH_3CN$  with 10 mM  $CCI_3CO_2H$ , 1 mm pathlength) with 50 mM  $H_2O_2$ . (c) Raman spectrum ( $\lambda_{exc}$  355 nm) before (black) showing resonantly enhanced bands of **1** at 700 cm<sup>-1</sup> and after addition of  $H_2O_2$  (500 mM, purple) with the non-resonantly enhanced O-O stretch of  $H_2O_2$  at 870 cm<sup>-1</sup>. The bands of **1** and  $H_2O_2$  decrease concomitant with the appearance of the resonantly enhanced band of **2** at 765 cm<sup>-1</sup>, reaching a maximum (light green) before decreasing also until all  $H_2O_2$  has been consumed (green). (d) Time dependence of Raman intensity for each of the bands indicated and the intensity of the solvent ( $CH_3CN$ ) band at 920 cm<sup>-1</sup> which decreases and increases concomitant with the appearance and loss of **2** due to inner filter effects. The changes in the intensity of this band correspond exactly to the changes in the UV/Vis absorption spectrum.

#### 8.3. Transient and time resolved resonance Raman spectroscopy

The recent increase in interest in photoredox catalysis has seen the widespread application of transition metal complexes and organic chromophores that can undergo photoexcitation and then

electron transfer with other species in solution. When Raman spectroscopy is carried out using a pulsed laser, i.e. a laser which delivers a packet of photons to the sample all within a few nanoseconds, then photoexcitation (excitation to meta stable excited states rather than virtual states) becomes significant (see Browne, et al. 2005, Browne, McGarvey, 2006, & 2007). If we consider the power (number of photons) as a function of time (see Figure 31), then we note that the first photons arriving at the sample will give some Raman scattering but also will excite the molecules into electronically excited states. The extent to which the molecules in the sample are excited depends on the intensity of the laser pulse (number of photons per unit time). If a significant proportion are in an electronically excited state then the photons which arrive later (i.e. within a ns or so) will generate Raman scattering from these excited molecules as well as molecules in the ground state. The relative contribution of Raman scattering from the molecules in the ground state and molecules in the excited state depends on the total number of photons arriving at the sample per unit time. Hence, at low power, relatively few molecules are excited electronically and the Raman scattering is weak (since the laser power is low). As a result, the Raman spectrum is close to that expected with a continuous wave (CW) laser used normally in Raman spectroscopy. If the energy per pulse is increased then the proportion of the sample that is excited will increase also and the Raman spectrum will become more intense overall (high laser power) and the contributions from Raman scattering from the molecules in the excited state will increase relative to molecules in the ground state. Changing the relative contributions from molecules in their electronic ground state and excited molecules by changing power is a relatively simple way to gain information on the electronic nature of the lowest excited states and the experiment is referred to as transient resonance Raman spectroscopy (TR<sup>2</sup>). The technique allows us to probe the nature of the lowest thermally equilibrated excited (THEXI) states and for example, in ruthenium(II) polypyridyl complexes, to determine whether they are metal to ligand charge transfer (3MLCT) states localized on one or other ligand. This information is important for understanding excited state behavior such as electron transfer, photo-dissociation etc.

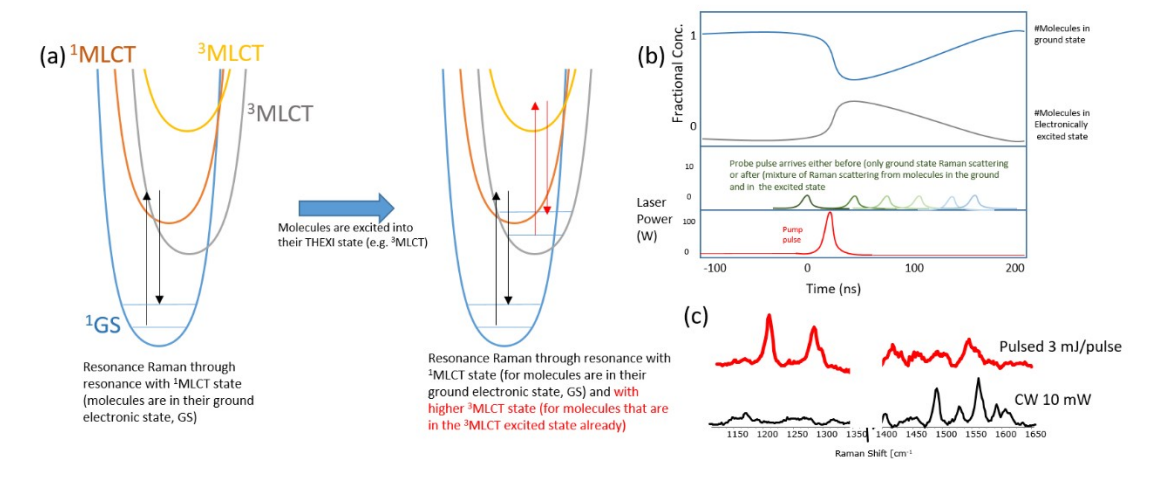


Figure 31. (a) Transient and time resolved Raman spectroscopy are based on exciting a significant number of molecules into their excited electronic state. The Raman spectrum acquired when these excited molecules are present will be a mixture of the Raman spectrum of the molecules in the ground state and the molecules in the excited state. (b) The ratio of the species can be changed by increasing the power of the pump pulse. The molecules relax back to their ground electronic state rapidly after the pump pulse has passed. (c) Example of resonance Raman spectra of a ruthenium(II) polypyridyl complex using a continuous wave laser (where the laser power is constant over time and very few molecules are present in their excited state) and a pulsed laser where all the light arrives

within a few nanoseconds in a 'packet' (and hence a large proportion of the molecules are excited into their electronically excited state). The pulsed laser also generates Raman scattering from the sample but since most molecules are in the excited state the Raman spectrum is dominated by these. In this case the excited state is a <sup>3</sup>MLCT state where formally one ligand has undergone a one-electron reduction and the bands at 1212 and 1285 cm<sup>-1</sup> are characteristic of such an anion radical.

The technique relies the molecule in the excited state also absorbing (is resonant) at the same wavelength as the laser used. If this is not the case then the excited molecule will be 'invisible' and the only effect increasing laser power will have is to cause a decrease in the intensity of the Raman scattering of the molecules in the ground state (relative to the solvent bands).

Since some compounds have relatively stable excited states that persist for several nano- or even micro-seconds then a two pulse experiment can give time dependent information. The first pulse arrives at the sample and promotes a part of the sample into its electronically excited state. A second pulse (either of the same or a different wavelength) that is weaker (so as not to disturb significantly the ratio of molecules in the ground and excited states) arrives at a set time after the first pulse and the Raman scattering generated by this pulse gives the spectrum. As the delay between the pulses increases the molecules have more and more time to relax back to the ground state and hence the spectrum will return eventually to that of the ground state only. In this way we are able to build up kinetic information as to the relaxation of the excited state.

#### 9. Conclusions

Although fundamentally a vibrational spectroscopy and hence providing information as to molecular structure, functional groups etc. in a manner complementary to FTIR spectroscopy, Raman spectroscopy has proven itself over nearly a century of practical and theoretical development to be a versatile and informative tool in the study of molecular systems and materials. The simplicity with which samples can be analyzed and the various mechanisms which allow us to enhance signals from particular species selectively make it unique. It is therefore understandable that the technique has something to offer in every field of chemical science. In this chapter, the phenomenon of resonance enhancement is addressed including an admittedly cursory consideration of the fundamental theory that underpins the technique. However, the main aim of the chapter is to impress upon the reader two key aspects. The first is that there is little by way of practical difference in recording resonance Raman spectra compared with recording a Raman spectrum. In fact, there is no such thing as a 'resonance Raman' spectrum and it is, in my view, unfortunate albeit unavoidable, that the term has crept into the lexicon of this field. What we in fact mean by the term is that the laser wavelength used coincides with an electronic absorption band of a component of a sample under study and as a result its Raman scattering is possibly orders of magnitude greater than would otherwise be expected for its concentration in the sample. For the rest it is just a Raman spectrum. The second and final point regards the interpretation of Raman spectra. At its most basic, we interpret a Raman spectrum in essentially the same manner as we interpret an FTIR spectrum (wavenumber, intensity, band shape etc.) but the technique offers much more than structural analysis and determination of concentration. It allows us to probe the behavior and interactions of molecules in real environments (no sample preparation) and extract information as to electronic structure in detail. Combined with theoretical methods therefore we have, through resonance enhancement, a unique window to the world of molecules in complex environments and it is perhaps biology that presents us with the most complex of bioinorganic environments.

#### 10. Questions

- 1. Sketch the Raman spectrum of air with excitation at 532 nm (consider Figure 28) showing both Stokes and anti-Stokes at 150 K and at 400 K.
- 2. What factors determine the extent of resonance enhancement that can be achieved by excitation into an electronic absorption band?
- 3. Why does the so called A-term in the KHD equation not contribute significantly to Raman intensity when the wavelength of excitation is not in resonance with an electronic transition.
- 4. In Figure 25, why do only some of the bands shift when Na<sup>18</sup>OCl is used instead of Na<sup>16</sup>OCl?
- 5. Why are only these Raman bands of the complexes the only bands observed in the spectra in Figure 25 whereas the spectrum of the complex in the Fe(II) oxidation state (Figure 24) shows many more bands in the range 200 -1600 cm<sup>-1</sup>.

#### **Answers**

1. The Raman spectrum of air is primarily comprised of the single stretching mode of O2 and of N<sub>2</sub> and 1553 cm<sup>-1</sup> and 2330 cm<sup>-1</sup> respectively. The ratio of Stokes and anti-Stokes depends on temperature and difference in energy of the first and second vibrational states. At 298 K the

ratio for oxygen is 
$$\frac{n_1}{n_0} = \exp\left(\frac{-1553\,cm^{-1}}{0.695\,cm^{-1}\,K^{-1}\times150\,K}\right) = 3.4\times10^{-7}$$
 and for nitrogen the ratio is  $\frac{n_1}{n_0} = \exp\left(\frac{-2330\,cm^{-1}}{0.695\,cm^{-1}\,K^{-1}\times150\,K}\right) = 2\times10^{-10}$  Hence the anti-Stokes scattering is 7-

ratio is 
$$\frac{n_1}{n_0} = \exp\left(\frac{-2330 \, cm^{-1}}{0.695 \, cm^{-1} \, K^{-1} \times 150 \, K}\right) = 2 \times 10^{-10}$$
 Hence the anti-Stokes scattering is 7-

10 orders of magnitude weaker than the Stokes scattering. Notably the ratio of the intensity of the  $N_2$  band to the  $O_2$  band is 6% that observed in the Stokes Raman spectrum. At 400 K the ratio between the N<sub>2</sub> and O<sub>2</sub> anti-Stokes bands is 0.06 that of the Stokes bands.

- The primary factor is the transition dipole moment for the electronic transition giving rise to enhancement. Hence d-d transitions give low enhancement while  $\pi$ - $\pi$ \* transitions give large enhancements.
- The A-term has the Frank-Condon factors in the numerator, the overlap between the vibrational wavefunctions in the ground and excited states,  $\langle \Phi_{R_s} | \Phi_{R_t} \rangle \langle \Phi_{R_t} | \Phi_{R_s} \rangle$ . If the potential wells of the ground and excited states are identical i.e. there is no difference in bond length (mean nuclear coordinates,  $\Delta Q > 0$ ) or force constant (bonds involved in the mode get either stronger or weaker,  $\Delta k > 0$ ) between the ground and excited electronic states, then this term is equal to zero (no-overlap) unless the ground and final states are the same. Hence, the A term contributes to polarizability primarily in the case of Rayleigh scattering.
- 4. Only bands which involve displacement of the oxygen atom will be shifted and hence the band at 673 cm<sup>-1</sup> is likely to be a mode involving for example Fe-N stretching.
- The absorption bands correspond to charge transfer to oxygen or metal centered transitions and hence only the bonds between Fe/Cl and oxygen and the nitrogen atoms are affected as they are the only bonds to change in equilibrium bond length and/or force constant (bond strength). These are prerequisites for resonance enhancement.

#### 11. Acknowledgements

The assistance of Prof. Doekele Stavenga, Tjalling Canrinus, Dr Davide Angelone, Ruben Feringa, Andy Sardjan, Dr Apparao Draksharapu and Dr Juan Chen in the collection of data used to prepare some of the figures and Dr Ronald Hage, Hanneke Siebe, Linda Eijsink, Hans Kasper, Andy Sardjan, and Jorn Steen for comments and suggestions is greatly appreciated and acknowledged. Prof Steven Bell and Prof John McGarvey (1939-2017) are acknowledged for general discussion.

#### 12. References

- A. C. Albrecht. On the Theory of Raman Intensities. J. Chem. Phys. 1961, 34, 1476.
- W. R. Browne, J. J. McGarvey. The Raman effect and its application to electronic spectroscopies in metal-centered species: Techniques and investigations in ground and excited states. Coord. Chem. Rev. 2007, 251, 454.
- W. R. Browne, J. J.McGarvey. Raman scattering and photophysics in spin-state-labile d<sup>6</sup> metal complexes. Coord. Chem. Rev. 2006, 250, 1696.
- W. R. Browne, N. M. O'Boyle, J. J. McGarvey, J. G. Vos. Elucidating excited state electronic structure and intercomponent interactions in multicomponent and supramolecular systems. Chem. Soc. Rev. 2005, 34, 641.
- R. S. Czernuszewicz, T. G. Spiro. In Inorganic electronic structure and spectroscopy; E. I. Solomon, A. B. P. Lever, Eds.; John Wiley & Sons: New York, 1999, Vol. I, pp 353-441.
- A. Draksharapu, Q. Li, H. Logtenberg, T. A. van den Berg, A. Meetsma, J. S. Killeen, B. L. Feringa, R. Hage, G. Roelfes, W. R. Browne. Ligand Exchange and Spin State Equilibria of Fe<sup>II</sup>(N4Py) and Related Complexes in Aqueous Media. *Inorg. Chem.* 2012, 51, 900.
- A. Draksharapu, A. J. Boersma, M. Leising, A. Meetsma, W. R. Browne, G. Roelfes. Binding of copper(II) polypyridyl complexes to DNA and consequences for DNA-based asymmetric catalysis. Dalton Trans. 2015, 44, 3647.
- A. Draksharapu, D. Angelone, M. G. Quesne, S. K. Padamati, L. Gómez, R. Hage, M. Costas, W. R. Browne, S P. de Visser. Identification and spectroscopic characterization of nonheme iron(III) hypochlorite intermediates. Angew. Chem., Int. Ed. 2015, 54, 4357.
- I. Drienovská, A. R.-Martínez, A. Draksharapu, G. Roelfes. Novel artificial metalloenzymes by in vivo incorporation of metal-binding unnatural amino acids. Chem. Sci. 2015, 6, 770.
- E. J. Heller. The semiclassical way to molecular spectroscopy. Acc. Chem. Res. 1981, 14, 368.
- P. J. Larkin. IR and Raman spectroscopy Principles and spectral interpretation. Elsevier, Oxford, UK, 2011.
- D. Long. The Raman effect; a unified treatment of the theory of Raman scattering by molecules, John Wiley &Sons, 1977.
- R. M. McCreery. Raman Spectroscopy for Chemical Analysis. John Wiley & Sons Ltd, New York, USA, 2000.
- F. Paulat, V. K. K. Praneeth, C. Näther, N. Lehnert, Quantum Chemistry-Based Analysis of the Vibrational Spectra of Five-Coordinate Metalloporphyrins [M(TPP)CI]. Inorg. Chem. 2006, 45, 2835.
- D. L. Rousseau, J. M. Friedman, P. F. Williams. Topics in Current Physics. 1979, 2, 203.
- E. Smith, G. Dent. Modern Raman Spectroscopy A Practical Approach, John Wiley & Sons Ltd, Chichester, UK, 2005.
- K. M. Van Heuvelen, A. T. Fiedler, X. Shan, R. F. De Hont, K. K. Meier, E. L. Bominaar, E Münck, L. Que Jr. One-electron oxidation of an oxoiron(IV) complex to form an [O=FeV=NR]<sup>+</sup> center. Proceed. Natl. Acad. Sci. 2012, 109, 11933.